

Chapter 2

Basic Equations of Atmospheric Turbulence

Before starting the derivation of the equations for the turbulent fluxes of momentum, heat and trace gases (Sect. 2.3), we present a short introduction into the basic equations. These include the equations of mean and turbulent motions, describing the transport and for energy and matter (Sect. 2.1), and the conservation equation for the turbulence kinetic energy (Sect. 2.2). To illustrate the importance of micrometeorological equations and parameterizations for modelling on all scales, different closure techniques of the turbulent differential equations are described (Sect. 2.1.3). The more practical user of this book can proceed directly to Sect. 2.3.

2.1 Equation of Motion

2.1.1 Navier-Stokes Equation of Mean Motion

The Navier-Stokes equations describe the balance of all the forces in the earth's atmosphere without consideration of the centrifugal force (Stull 1988; Arya 1999; Etling 2008; Wyngaard 2010; Hantel 2013):

$$\begin{aligned}
 \frac{\partial u}{\partial t} &= -u \frac{\partial u}{\partial x} - v \frac{\partial u}{\partial y} - w \frac{\partial u}{\partial z} - \frac{1}{\rho} \frac{\partial p}{\partial x} + f v + \nu \nabla^2 u \\
 \frac{\partial v}{\partial t} &= -u \frac{\partial v}{\partial x} - v \frac{\partial v}{\partial y} - w \frac{\partial v}{\partial z} - \frac{1}{\rho} \frac{\partial p}{\partial y} - f u + \nu \nabla^2 v \\
 \frac{\partial w}{\partial t} &= -u \frac{\partial w}{\partial x} - v \frac{\partial w}{\partial y} - w \frac{\partial w}{\partial z} + g + \nu \Delta w
 \end{aligned}
 \tag{2.1}$$

where u is the horizontal wind in the x -direction (east); v is the horizontal wind in the y -direction (north), and w is the vertical wind; p is the atmospheric pressure; f is the Coriolis parameter; g is the gravity acceleration; ρ is the air density; ν is the

Table 2.1 Definitions of Einstein's summation notation

Running index of the velocity components	$i = 1, 2, 3$ $u_1 = u$	$j = 1, 2, 3$ $u_2 = v$	$k = 1, 2, 3$ $u_3 = w$
Length components	$x_1 = x$	$x_2 = y$	$x_3 = z$
Variables	No free index: scalar	One free index: vector	Two free indexes: tensor
Kronecker delta-operator δ_{ij}	= +1, for $i = j$	= 0, for $i \neq j$	
Levi-Civita symbol (alternating unit tensor) ε_{ijk}	= +1, for $ijk = 123, 231$ or 312	= -1, for $ijk = 321, 213$ or 132	= 0, for $ijk =$ all other combinations

kinematic viscosity, and ∇^2 is the Laplace operator. From left-to-right, the terms of the equation are the tendency, the advection, the pressure gradient force, the Coriolis force, and the (molecular) stress. In a turbulent atmosphere, a turbulent stress term, the Reynolds stress, must be applied. All the terms in the horizontal motion equations are of the order of $10^{-4} - 10^{-3} \text{ m s}^{-2}$. Under certain condition, some terms are very small and can be neglected. For example, for steady-state flow, the tendency can be neglected; above horizontally homogeneous surfaces, the advection can be neglected; in the centre of high and low pressure areas or for small scale processes the pressure gradient force can be neglected; at the equator or for small scale processes the Coriolis force can be neglected, and above the atmospheric boundary layer the stress terms can be neglected.

The three equations of the wind components can be combined applying Einstein's summation notation and partial derivatives:

$$\frac{\partial u_i}{\partial t} = -u_j \frac{\partial u_i}{\partial x_j} - \delta_{i3}g + f\varepsilon_{ij3}u_j - \frac{1}{\rho} \frac{\partial p}{\partial x_i} + \frac{1}{\rho} \left(\frac{\partial \tau_{ij}}{\partial x_j} \right) \quad (2.2)$$

The shear stress tensor with dynamic viscosity μ is given in the form (Stull 1988):

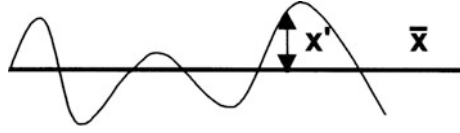
$$\tau_{ij} = \mu \left(\frac{\partial u_i}{\partial x_j} + \frac{\partial u_j}{\partial x_i} \right) - \frac{2}{3} \mu \frac{\partial u_k}{\partial x_k} \delta_{ij} \quad (2.3)$$

The generalizations and applications of the Einstein summation operators are summarized in Table 2.1.

2.1.2 Turbulent Equation of Motion

The modification of the Navier-Stokes equations to include turbulent motions requires the decomposition of all the variables into a mean part, \bar{x} , and a random

Fig. 2.1 Schematic presentation of Reynolds's decomposition of the value x



fluctuating part, x' . This is called the Reynolds's decomposition (Fig. 2.1), and is represented by:

$$x = \bar{x} + x'. \quad (2.4)$$

The application of Reynolds's decomposition requires some averaging rules for the turbulent value x' and y' (a represents a constant), which are termed Reynolds's postulates:

$$\begin{aligned} \text{I} \quad & \overline{x'} = 0 \\ \text{II} \quad & \overline{x'y} = \bar{x}\bar{y} + \overline{x'y'} \\ \text{III} \quad & \overline{\bar{x}y} = \bar{x}\bar{y} \\ \text{IV} \quad & \overline{ax} = a\bar{x} \\ \text{V} \quad & \overline{x+y} = \bar{x} + \bar{y} \end{aligned} \quad (2.5)$$

It is assumed that the postulates are universal, but for special spectral regions or for intermitted turbulence this is not valid (Bernhardt 1980). The second postulate is the basis for the determination of turbulent fluxes according to the direct eddy-covariance method (see Sect. 4.2).

The turbulent equations of motion follow after application of Reynolds's decomposition and postulates into Eq. (2.2). It is also assumed (Businger 1982; Stull 1988), that:

$$\begin{aligned} |p'/\bar{p}| &\ll |\rho'/\bar{\rho}| \\ |p'/\bar{p}| &\ll |T'/\bar{T}| \\ |\rho'/\bar{\rho}| &\ll 1 \\ |T'/\bar{T}| &\ll 1 \end{aligned} \quad (2.6)$$

These assumptions are not trivial and need further inspections for individual cases. A very important simplification results from the Boussinesq-approximation (Boussinesq 1877), which neglects density fluctuations except for the buoyancy (gravitation) term. This is because the acceleration of gravity is relatively large in comparison with the other accelerations in the equation. Therefore, shallow convective conditions (Stull 1988) are permitted. This form of averaging is not without consequences for the determination of turbulent fluxes (see Sect. 4.2.3). Applying all these simplifications it follows that:

$$\frac{\partial \overline{u_i}}{\partial t} + \frac{\partial}{\partial x_j} (\overline{u_j u_i} + \overline{u'_j u'_i}) = -\frac{1}{\rho} \frac{\partial \overline{p}}{\partial x_i} + \nu \frac{\partial^2 \overline{u_i}}{\partial x_i^2} + g \delta_{i3} + \varepsilon_{ijk} f \overline{u_k} \quad (2.7)$$

Completely analogous equations for the heat transfer and the transfer of trace gases such as water vapour can be derived

$$\frac{\partial \overline{T}}{\partial t} + \frac{\partial}{\partial x_i} (\overline{u_i T} + \overline{u'_i T'}) = a_T \frac{\partial^2 \overline{T}}{\partial x_i^2} + R, \quad (2.8)$$

$$\frac{\partial \overline{c}}{\partial t} + \frac{\partial}{\partial x_i} (\overline{u_i c} + \overline{u'_i c'}) = D \frac{\partial^2 \overline{c}}{\partial x_i^2} + S, \quad (2.9)$$

where R and S are source and sink terms respectively, and a_T and D are the molecular heat conduction and diffusion coefficients, respectively.

An important simplification is possible in the atmospheric boundary layer where only the equations for $j = 3$, i.e. $u_3 = w$, are important, and steady state conditions ($\partial/\partial t = 0$) and horizontal homogeneity ($\partial/\partial x_1 = 0$, $\partial/\partial x_2 = 0$) are assumed. This assumption is far reaching because all the following applications are valid only under these conditions. For instance, for all micrometeorological measurements steady state conditions are implied (see Sect. 4.2.4), and a mostly homogeneous surface is necessary. Under these assumptions and including the components u_g and v_g of the geostrophic wind velocity and the angular velocity of the earth's rotation, Ω , the three equations of motion become:

$$\frac{\partial \overline{u'w'}}{\partial z} = f(\overline{v} - \overline{v_g}) + \nu \frac{\partial^2 \overline{u}}{\partial z^2}, \quad \overline{v_g} = \frac{1}{\rho f} \frac{\partial \overline{p}}{\partial x} \quad (2.10)$$

$$\frac{\partial \overline{v'w'}}{\partial z} = -f(\overline{u} - \overline{u_g}) + \nu \frac{\partial^2 \overline{v}}{\partial z^2}, \quad \overline{u_g} = -\frac{1}{\rho f} \frac{\partial \overline{p}}{\partial y} \quad (2.11)$$

$$\frac{\partial \overline{w'^2}}{\partial z} = \frac{1}{\rho} \frac{\partial \overline{p}}{\partial z} - g - 2[\Omega_u \overline{v} - \Omega_v \overline{u}], \quad f = 2 \Omega \sin \varphi \quad (2.12)$$

Equations (2.10) and (2.11) are the basis of the so-called ageostrophic method for the determination of the components of the shear stress tensor using differences between the wind velocity in the atmospheric boundary layer and the geostrophic wind (Lettau 1957; Bernhardt 1970). The practical application of the ageostrophic method is limited because of baroclinicity, nonsteady-state conditions, and inhomogeneities (Schmitz-Peiffer et al. 1987). For example, they can be applied only for the determination of the shear stress at the ground surface using a large number of aerological observations (Bernhardt 1975).

In addition, the continuity equation in the incompressible form is assumed:

$$\frac{\partial \bar{u}_i}{\partial x_i} = 0, \quad \frac{\partial \bar{w}}{\partial z} = 0, \quad \bar{w} = 0 \quad (2.13)$$

The gas law with the specific gas constant for dry air R_L and the virtual temperature T_v (temperature of the dry air, which has the same density as the moist air)

$$T_v = T(1 + 0.61 \cdot q), \quad (2.14)$$

with the specific humidity q , completes the system of equations:

$$p = \rho R_L T_v \quad (2.15)$$

In an analogous way, the equations for heat and trace gas transfer are:

$$\frac{\partial \overline{w'T'}}{\partial z} = a_T \frac{\partial^2 \bar{T}}{\partial z^2}, \quad \text{for } R = 0 \quad (2.16)$$

$$\frac{\partial \overline{w'c'}}{\partial z} = D \frac{\partial^2 \bar{c}}{\partial z^2}, \quad \text{for } S = 0 \quad (2.17)$$

The influence of the individual terms in the different layers of the atmospheric boundary layer can be estimated using similarity numbers. These numbers are dimensionless values describing the relations between characteristic scales of the forces. Two physical systems are similar if the similarity numbers of both systems are on the same order. This is imported if atmospheric processes are investigated in a wind tunnel or water channel.

The ratio of the inertia to the pressure gradient force is called the Euler number

$$Eu = \frac{\rho V^2}{\Delta P}, \quad (2.18)$$

where V is the characteristic velocity, and ΔP is the characteristic pressure gradient.

The ratio of the inertia force to the Coriolis force is the Rossby number

$$Ro = \frac{V}{f L_h}, \quad (2.19)$$

where L_h is the characteristic large-area horizontal length scale.

The ratio of the inertia force to the molecular stress is the Reynolds number

$$Re = \frac{L_z V}{\nu}, \quad (2.20)$$

where L_z is the characteristic small-scale vertical length scale.

The ratio of the buoyancy production or destruction (stratification of the atmosphere) to the shear production of turbulence kinetic energy is the Richardson flux number (see Sect. 2.3.3). A bulk Richardson number can be defined as

$$Ri = -\frac{g}{T} \frac{\Delta_z T \Delta_z}{(\Delta_z u)^2}, \quad (2.21)$$

where $\Delta_z T$ is the characteristic temperature gradient, and $\Delta_z u$ is the characteristic vertical wind gradient (see Sect. 2.3.2).

For heights above 10 m the temperature must be replaced by the potential temperature θ . Due to the decrease of atmospheric pressure with height it follows from Poisson's equation (Kraus 2004; Salby 2012):

$$\theta = T \left(\frac{1000}{p} \right)^{R_L/c_p} \quad (2.22)$$

Replacing potential by air temperature is only valid for heights below 10 m resulting in errors of less than 0.1 K.

The relevant processes in the atmospheric boundary layer can be identified using dimensional analysis and the similarity numbers. Using the logarithms of the similarity numbers the relevant processes can be identified for logarithms smaller than zero (Bernhardt 1972) as listed in Table 2.2. From the structure of the atmospheric boundary layer presented in Fig. 1.4, this is a logical organization.

It can be shown that the pressure gradient force is important only in the upper boundary layer. Molecular viscosity is only relevant in the viscous and molecular sub-layer. The effect of the Coriolis force can be neglected in the flux gradient relationships (see Sect. 2.3) in the surface layer, but not in general (see Sect. 2.4). On the other hand, the turbulent stress is relevant in the whole boundary layer.

In the dynamical and viscous sub-layers, the stratification does not play a role. Under these circumstances, it is possible that the vertical gradients are nearly zero:

Table 2.2 Order of the similarity numbers in the layers of the atmospheric boundary layer (**bold**: Processes characterized by the similarity numbers are relevant)

Layer	Height	lg Ro	lg Eu	lg Re	lg $ Ri $
Upper layer	~1000 m	<0	<0	>0 $Re > 10^8$	> -2
Surface layer	~10 ... 50 m	~0	<0	>0 $Re \sim 10^7 \dots 10^8$	> -2
Dynamical sub-layer	~1 m	>0	~0	>0 $Re < 10^7$	~ -2
Viscous sub-layer	~0.01 m	>0	>0	~0	< -2
Molecular or laminar boundary layer	~0.001 m	>0	>0	<0	< -2

$$\frac{\partial \overline{u'w'}}{\partial z} \approx 0, \quad \frac{\partial \overline{v'w'}}{\partial z} \approx 0, \quad \frac{\partial \overline{T'w'}}{\partial z} \approx 0, \quad \frac{\partial \overline{c'w'}}{\partial z} \approx 0 \quad (2.23)$$

These equations mean that the covariances are constant with height in the surface layer. An error in this assumption of approximately 10% is typical.

The covariance of the vertical wind velocity, w , and a horizontal wind component or a scalar x can be determined by:

$$\begin{aligned} \overline{w'x'} &= \frac{1}{N-1} \sum_{k=0}^{N-1} [(w_k - \overline{w}_k) (x_k - \overline{x}_k)] \\ &= \frac{1}{N-1} \left[\sum_{k=0}^{N-1} w_k \cdot x_k - \frac{1}{N} \left(\sum_{k=0}^{N-1} w_k \sum_{k=0}^{N-1} x_k \right) \right] \end{aligned} \quad (2.24)$$

According to the second Reynolds's postulate (Eq. 2.5, II), in the case of a negligible vertical wind the total flux is equal to the covariance. This equation is implemented in the eddy-covariance method, a method to directly measure turbulent fluxes (see Sect. 4.2). The dimensions of the turbulent fluxes of momentum (expressed as square of the friction velocity), sensible and latent heat, and matter are in kinematic units $\text{m}^2 \text{s}^{-2}$, K m s^{-1} , and $\text{kg kg}^{-1} \text{m s}^{-1}$, respectively. For water vapour flow, the units are hPa m s^{-1} :

$$u_*^2 = -\overline{u'w'}, \quad \frac{Q_H}{\rho \cdot c_p} = \overline{T'w'}, \quad \frac{Q_E}{\rho \cdot \lambda} = \overline{q'w'}, \quad \frac{Q_c}{\rho} = \overline{c'w'} \quad (2.25)$$

The equation for the friction velocity is valid only if u is the direction of the mean wind velocity. This simplification is typically used in micrometeorology and is equivalent to a coordinate rotation around the z -axis (see Sect. 4.2.3). The covariance of u' and w' is negative except below the crown in a forest (Amiro 1990). For a Cartesian coordinate system that is not aligned with the flow streamlines the friction velocity is given by:

$$u_* = \left[(\overline{u'w'})^2 + (\overline{v'w'})^2 \right]^{1/4} \quad (2.26)$$

The friction velocity is a generalized velocity, i.e., it is the shear stress divided by the density

$$u_* = \sqrt{\frac{\tau}{\rho}}. \quad (2.27)$$

2.1.3 Closure Techniques

The transition from the equation of motion from mean to turbulent flow gives a system of differential equations with more unknown parameters than equations. To solve the system of equations, assumptions have to be made to calculate the unknown parameters. These assumptions, for example for the covariance terms, are called closure techniques.

The order of the closure refers to the highest order of the parameters that must be calculated with the prognostic equations. Therefore, the moments of the next higher order must be determined (Table 2.3). Simple closure techniques are bulk approaches (see Sect. 4.1.1). Closer techniques of higher order require extensive calculations (Table 2.4). The most important approaches are presented here.

2.1.3.1 Local or first-order closure

First-order closure is analogous to molecular diffusion approaches, i.e. an assumed proportionality between the vertical flux and the vertical gradient of the relevant state parameter ξ . In the turbulent case, the proportionality factor is the eddy diffusion coefficient, K , and the approach is called K -theory. The gradient will be determined at the same place where the flux is to be calculated; therefore it is a local closure:

$$\overline{u'_i \xi'} = -K \frac{\partial \bar{\xi}}{\partial z} \quad (2.28)$$

The product of air density and turbulent diffusion coefficient (Eq. 1.22) is called “Austausch”-coefficient or exchange coefficient. The turbulent diffusion coefficients

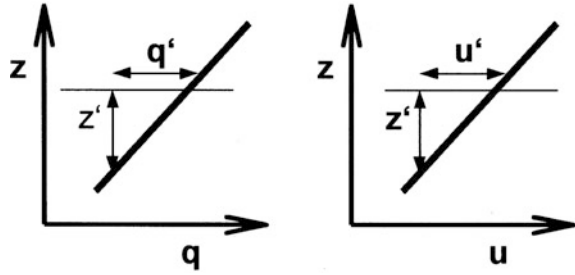
Table 2.3 Characterization of closure techniques (Stull 1988)

Order of closure	Prognostic equation for	To be approximate in the equation	Number of equations	Number of unknown parameters
1st order	\bar{u}_i	$\bar{u}_i u_j$	3	6
2nd order	$\bar{u}_i u_j$	$\bar{u}_i u_j u_k$	6	10
3rd order	$\bar{u}_i u_j u_k$	$\bar{u}_i u_j u_k u_l$	10	15

Table 2.4 Realization of closure techniques

Order of closure	Realization
0. order	No prognostic equation (bulk and similarity approaches)
½ order	Forecast with simple bulk approaches
1. order	K -approach (local) Transilient closure (non-local)
1½ order	TKE equation with variance terms
2. order	Prognostic equation for fluxes
3. order	Prognostic equation for triple correlations

Fig. 2.2 Schematic view of the movement of an air parcel z' to explain the mixing length approach



are formed for momentum, sensible heat, water vapour (latent heat), etc. For the single fluxes in kinematic units, the following relations are used:

$$\overline{u'w'} = K_m \frac{\partial \bar{u}}{\partial z} \tag{2.29}$$

$$\overline{w'T'} = -K_H \frac{\partial \bar{T}}{\partial z} \tag{2.30}$$

$$\overline{w'q'} = -K_E \frac{\partial \bar{q}}{\partial z} \tag{2.31}$$

For the determination of the turbulent diffusion coefficients, the mixing length parameterization is used, which is based on the work of Prandtl (1925). This approach describes the turbulent diffusion coefficient in terms of geometric and flux parameters. This is illustrated in the following example for the moisture flux. If an air parcel moves to a slightly different height, it will have a humidity and velocity slightly different than its new environment. This change of the environmental velocity and humidity can be described with gradients (Fig. 2.2):

$$u' = -\left(\frac{\partial \bar{u}}{\partial z}\right) z' \quad q' = -\left(\frac{\partial \bar{q}}{\partial z}\right) z' \tag{2.32}$$

The vertical velocity, which is necessary for the movement of the parcel, is assumed proportional to the horizontal velocity (c : constant factor):

$$w' = \pm c u' = c \left| \frac{\partial \bar{u}}{\partial z} \right| z' \tag{2.33}$$

The water vapour flux and the turbulent diffusion coefficient for evaporation are then given by

$$\overline{w'q'} = -c \overline{(z')^2} \left| \frac{\partial \bar{u}}{\partial z} \right| \cdot \left(\frac{\partial \bar{q}}{\partial z} \right) = -l^2 \left| \frac{\partial \bar{u}}{\partial z} \right| \cdot \left(\frac{\partial \bar{q}}{\partial z} \right), \tag{2.34}$$

$$K_E = l^2 \left| \frac{\partial \bar{u}}{\partial z} \right|, \quad (2.35)$$

where l is called the mixing length. The mixing length is usually assumed to be

$$l = \kappa z, \quad (2.36)$$

where κ is the von-Kármán constant and z is the height above the ground surface. The value of κ is currently taken to be 0.4 (see Sect. 2.3.3).

The turbulent diffusion coefficient of momentum is:

$$K_m = \kappa^2 z^2 \left[\left(\frac{\partial \bar{u}}{\partial z} \right)^2 + \left(\frac{\partial \bar{v}}{\partial z} \right)^2 \right]^{1/2} \quad (2.37)$$

With Eqs. (2.24) and (2.28), the widely used exchange approach (K -approach) for neutral stratification in the surface layer is:

$$K_m = \kappa z u_* \quad (2.38)$$

Applications of local closure for the stratified surface layer are discussed in Sect. 2.3.3. Outside of the surface layer, closure parameterizations for greater heights in the atmospheric boundary layer are used (see Sect. 2.6.2). The K -theory approach can be always applied when the exchange process takes place between direct neighbouring atmospheric layers or turbulence elements. K -theory cannot be applied in convective boundary layers (i.e. the daytime mixed layer). Also, K -theory should not be used within high vegetation (see Sect. 3.5) or for very stable stratification (see Sect. 3.7).

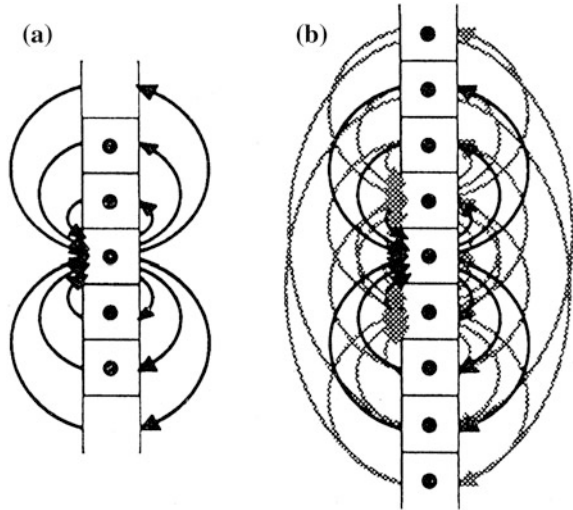
2.1.3.2 Non-local first-order closure

Local scaling approaches are no longer sufficient once larger eddies contribute to the exchange process, resulting in an overall flux that is greater than the flux due to the smaller eddies alone. This is e.g. the case for turbulent transport processes in tall vegetation and convective boundary layers. Possible solutions are given by either the transilient theory or the spectral diffusion theory.

The transilient theory (Stull 1984) approximates the turbulent exchange process between adjoining atmospheric layers or boxes, and also admits the exchange between non-adjoining boxes. The change of a scalar ξ with time in a box i is given by a fixed matrix of exchange coefficients, c_{ij} between the boxes i and j and the size of the scalar in the box j :

$$\bar{\xi}_i(t + \Delta t) = \sum_{j=1}^N c_{ij}(t, \Delta t) \bar{\xi}_j(t) \quad (2.39)$$

Fig. 2.3 Schematic view of the mixing of eddies from the central layer (a) and by superposition of similar mixing of the three layers in the centre (b) (Adapted from Stull 1988, with kind permission of © Kluwer Academic Publisher B. V. Dordrecht 1988, All rights reserved)



The matrix of mixing coefficients is called a transient matrix. The flux in the k -layer is given by:

$$\overline{w'\xi'}(k) = \left(\frac{\Delta z}{\Delta t}\right) \sum_{i=1}^k \sum_{j=1}^N c_{ij}(\overline{\xi}_i - \overline{\xi}_j) \tag{2.40}$$

Figure 2.3 illustrates the possibilities for mixing between boxes. In principle all possibilities of mixing can be realized by the definition of the transient matrix, which must be parameterized using external parameters such as the wind field or the radiation (Stull 1988). The difficulties of getting these parameters are the reasons why this form of the closure is rarely used.

2.1.3.3 Higher order closure

Closures higher than first order are now quite typical. But most of the parameterizations are poorly validated against observations. Commonly used, is a closure of 1.5th order. This is a closure using variances, which can be partially determined with the equation of the turbulence kinetic energy (TKE, see Sect. 2.2). 2nd order closure approaches use triple correlations (see Table 2.4).

2.2 Equation of the Turbulence Kinetic Energy

The equation of the turbulence kinetic energy, (TKE) in kinematic form is obtained by multiplication of the Navier-Stokes equation for turbulent flow Eq. (2.7) with u_i' . With the kinetic energy defined as (Stull 1988; Etling 2008; Wyngaard 2010)

Table 2.5 Meaning of the terms of the TKE equation

Term	Process
I	Local TKE storage or tendency
II	TKE advection
III	Buoyancy production or consumption
IV	Product from momentum flux (<0) and wind shear (>0) mechanical (or shear) production or loss term of turbulent energy
V	Turbulent TKE transport
VI	Pressure correlation term
VII	Energy dissipation

$$\bar{\epsilon} = 0.5 \left(\overline{u'^2} + \overline{v'^2} + \overline{w'^2} \right) = 0.5 \overline{u_t'^2} \quad (2.41)$$

it follows:

$$\frac{\partial \bar{\epsilon}}{\partial t} = \underbrace{-\bar{u}_j \frac{\partial \bar{\epsilon}}{\partial x_j}}_{\text{I}} + \underbrace{\delta_{i3} \frac{g}{\theta_v} \left(\overline{u'_i \theta'_v} \right)}_{\text{III}} - \underbrace{\bar{u}'_i u'_j \frac{\partial \bar{u}_i}{\partial x_j}}_{\text{IV}} - \underbrace{\frac{\partial \left(\overline{u'_j \epsilon'} \right)}{\partial x_j}}_{\text{V}} - \underbrace{\frac{1}{\rho} \frac{\partial \left(\overline{u'_i p'} \right)}{\partial x_i}}_{\text{VI}} - \underbrace{\epsilon}_{\text{VII}} \quad (2.42)$$

Descriptions of the terms in Eq. (2.42), which are in the order of $10^{-4} \text{ m}^2 \text{ s}^{-3}$, are given in Table 2.5. The changes of the magnitudes of the terms in Eq. (2.42) with height in the boundary layer are shown in Fig. 2.4, whereby the terms are normalized by $w_*^3 z_i^{-1}$ (order $6 \cdot 10^{-3} \text{ m}^2 \text{ s}^{-3}$). In a boundary layer that is strongly influenced by convective processes, the terms are usually normalized by the characteristic convective or Deardorff velocity (Deardorff 1970):

$$w_* = \left[\frac{g \cdot z_i}{\theta_v} \left(\overline{w' \theta'_v} \right) \right]^{1/3} \quad (2.43)$$

By application of the Obukhov-length L (see Sect. 2.3.3) it follows

$$w_* \approx 0,7 u_* \left(-\frac{z_i}{L} \right)^{1/3}, \quad (2.44)$$

while the conditions of free convection are given for $-z_i/L < -5 \dots 10$ (Wyngaard 2010).

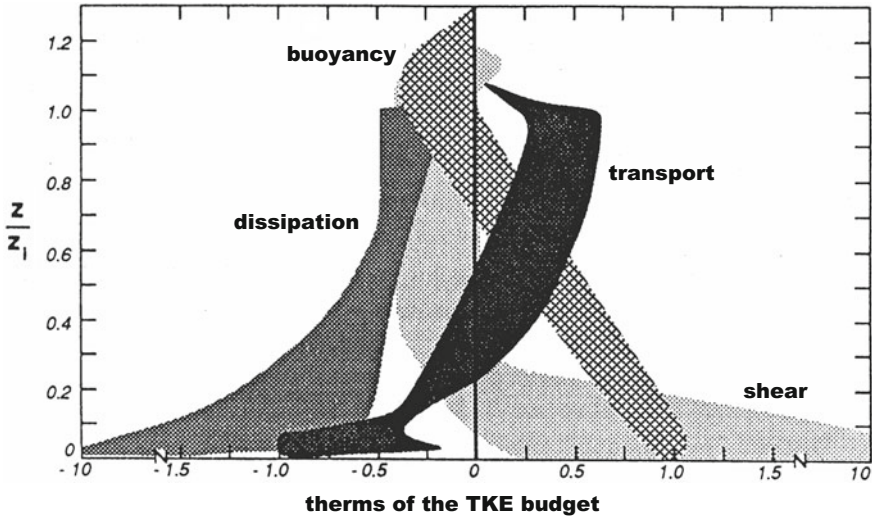


Fig. 2.4 Order of the terms of the TKE equation in the atmospheric boundary layer at daytime (Stull 1988) normalized with $w_*^3 z_i^{-1}$ (about $6 \times 10^{-3} \text{ m}^2 \text{ s}^{-3}$) (Adapted from Stull 1988, with kind permission of © Kluwer Academic Publisher B. V. Dordrecht 1988, All rights reserved)

Convection is the vertical transport or mixing of properties of the air (horizontal transport: advection). Forced convection results from mechanical forces (wind field) and inhomogeneities of the ground surface. It occurs for $1 > z/L > -1$ and appropriate scaling parameters are u_* and T_* . In contrast, free convection is caused by density differences and occurs for $z/L < -1$, and the scaling parameter is w_* . The fluxes in the case of free convection are typically not proportional to the local gradient (in the literature this is often referred to as counter gradient fluxes, Deardorff 1966).

Comparing the magnitudes of the terms of the TKE equation near the surface, terms I, II, V, and VI can be neglected relative to terms III, IV, and VII. The resulting equation is:

$$0 = \delta_{i3} \frac{g}{\theta_v} \left(\overline{u'_i \theta'_v} \right) - \overline{u'_i u'_j} \frac{\partial \overline{u}_i}{\partial x_j} - \varepsilon \tag{2.45}$$

This equation can be used in the surface layer to determine the energy dissipation ε , i.e., the decay of turbulent eddies into heat:

$$\varepsilon = \frac{g}{\theta_v} \left(\overline{w' \theta'_v} \right) - \overline{w' u'} \frac{\partial \overline{u}}{\partial z} \tag{2.46}$$

2.3 Flux-Gradient Similarity

2.3.1 Profile Equations for Neutral Stratification

In Sect. 2.1.3.1, it was shown that the flux could be determined by the vertical gradient of the state variable and a diffusion coefficient. These relations are called flux-gradient similarities. Thus, the turbulent diffusion coefficient for momentum can be parameterized in a simple way using Eq. (2.38). For the shear stress, it follows:

$$\tau = \rho K_m \frac{\partial u}{\partial z} \quad (2.47)$$

As discussed above, the friction velocity Eq. (2.26), is often used instead of the shear stress.

The turbulent fluxes of momentum, Eq. (2.29), sensible heat, Eq. (2.30), and latent heat, Eq. (2.31), can be calculated using the turbulent diffusion coefficient for momentum in the case of neutral stratification, Eq. (2.38), as the profile equations:

$$u_* = \sqrt{-\overline{u'w'}} = \kappa \cdot z \cdot \frac{\partial u}{\partial z} = \kappa \cdot \frac{\partial u}{\partial \ln z} \quad (2.48)$$

$$\overline{w'T'} = -\kappa \cdot u_* \cdot \frac{1}{Pr_t} \frac{\partial T}{\partial \ln z} \quad (2.49)$$

$$\overline{w'q'} = -\kappa \cdot u_* \cdot \frac{1}{Sc_t} \frac{\partial q}{\partial \ln z} \quad (2.50)$$

In Eq. (2.48) the friction velocity was defined in a simplified way in comparison to Eq. (2.26) by using the mean horizontal wind u . This first-order approximation is possible in the case of small wind fluctuations as shown by (Foken 1990).

Because the diffusion coefficients for momentum, sensible and latent heat are not identical, the turbulent Prandtl number Pr_t and the turbulent Schmidt number Sc_t are introduced. The turbulent Prandtl number is

$$Pr_t = \frac{K_m}{K_H}, \quad (2.51)$$

which is $Pr_t \sim 0.8$ for air (see Table 2.6). This definition is analogous to the Prandtl number of molecular exchange conditions

$$Pr = \frac{\nu}{\nu_T}, \quad (2.52)$$

with the thermal diffusion coefficient ν_T .

Table 2.6 Turbulent Prandtl number according to different authors

Author	Pr_t
Businger et al. (1971)	0.74
• Correction according to Wieringa (1980)	1.00
• Correction according to Högström (1988)	0.95
Kader and Yaglom (1972)	0.72–0.87
Foken (1990)	0.80
Högström (1996)	0.92 ± 0.03

Similarly, for the latent heat flux the Schmidt number

$$Sc = \frac{\nu}{D}, \quad (2.53)$$

of the molecular diffusion coefficient for water vapour, D , and the turbulent Schmidt number are applied:

$$Sc_t = \frac{K_m}{K_E} \quad (2.54)$$

For the latent heat flux (water vapour flux) and the matter flux the turbulent diffusion coefficients for heat are applied, even when this is not fully justified. The turbulent Prandtl- and Schmidt numbers can be determined only by the comparisons of profile measurements (see Sect. 4.1) and flux measurements with the eddy-covariance method (see Sect. 4.2) for neutral conditions. Because of the inaccuracies in these methods the coefficients contain remarkable errors and for the turbulent Schmidt number the same values as for the turbulent Prandtl number are applied. Table 2.6 gives an overview of the currently available data.

Transferring the given equations in kinematic units into energetic units requires multiplication by the air density, which can be determined according to the ideal gas law and either the specific heat for constant pressure c_p (for sensible heat flux) or the latent heat of evaporation λ (for latent heat flux). These values are temperature and pressure dependent (see Appendix A.3):

$$\rho = \frac{p[\text{hPa}] \cdot 100}{R_L \cdot T_v} \quad [\text{kg m}^{-3}] \quad (2.55)$$

$$c_p = 1004.834 \quad [\text{J K}^{-1} \text{kg}^{-1}] \quad (2.56)$$

$$\lambda = 2500827 - 2360(T - 273.15 \text{ K}) \quad [\text{J kg}^{-1}] \quad (2.57)$$

If the kinematic latent heat flux was based on water vapour pressure data, an additional correction factor of $0.62198/p$ (p in hPa) must be applied that accounts for the conversion into specific humidity in kg kg^{-1} . To achieve an accuracy better than 1% of the fluxes, the temperature must be determined with an accuracy of 1 K

and the pressure should be determined as a mean value with the barometric equation (Supplement 2.1) for the height above sea level. The following transformation relations are given:

$$\begin{aligned} Q_H[\text{W m}^{-2}] &= c_p \rho \overline{w'T'}[\text{K m s}^{-1}] \\ &= 1004.832 \frac{p[\text{hPa}] \cdot 100}{287.0586 \cdot T} \overline{w'T'}[\text{K m s}^{-1}] \end{aligned} \quad (2.58)$$

$$\begin{aligned} Q_E[\text{W m}^{-2}] &= \rho \lambda \overline{w'q'}[\text{kg kg}^{-1} \text{ m s}^{-1}] \\ &= \frac{p[\text{hPa}] \cdot 100}{287.0586 T} \frac{0.62198}{p[\text{hPa}]} [2500827 - 2360 (T - 273.15 \text{ K})] \\ &\quad \cdot \overline{w'e'}[\text{hPa m s}^{-1}] \end{aligned} \quad (2.59)$$

Supplement 2.1 Barometric equation

The pressure at some height Z can be calculated from the pressure at sea level $p(Z = 0)$ and the mean virtual temperature, T_v , between sea level and Z ,

$$p(Z) = p(Z = 0) e^{\frac{g_0}{R_L T_v} Z}, \quad (\text{S2.1})$$

where T_v is given by Eq. (2.14). Z is the geopotential height (Stull 2000), i.e. the geopotential Φ normalized with the constant gravity acceleration $g_0 = 9.81 \text{ m s}^{-2}$ (Hantel 2013),

$$Z = \frac{\Phi}{g_0}, \quad (\text{S2.2})$$

In the lower troposphere, the geopotential height differs only slightly from the geometric height. Also, depending on the required accuracy the virtual temperature can be replaced by the actual temperature.

For hydrological applications the latent heat flux is often converted into the evaporated amount of water with the evaporation equivalent (0.0347 mm d^{-1} are equal to 1 Wm^{-2} as the daily average).

The profile equations Eqs. (2.48)–(2.50) give the opportunity to determine the fluxes in a simple way using either semi-log paper or similar computer outputs as shown in Fig. 2.5. Such graphs are helpful for a quick check of the measurement results or the functioning of the sensors. An overview of applicable humidity units is given in Supplement 2.2. Relative humidity observations should never be used for computing latent heat fluxes. When converting relative humidity into other humidity variables, air temperature observations are needed, which can lead to cross-correlations between latent and sensible heat fluxes. For heights above 10 m potential temperature (Eq. 2.22) instead of air temperature must be used.

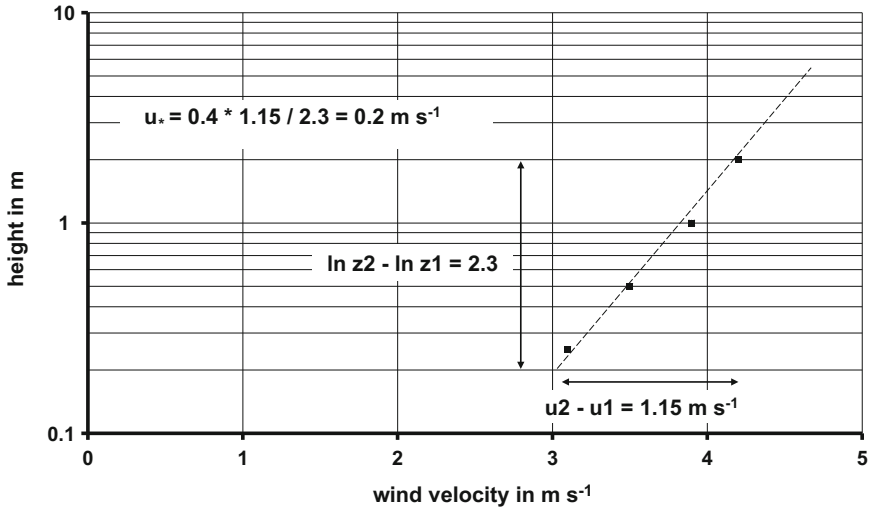


Fig. 2.5 Determination of the friction velocity from the wind profile with a semi-log plot

Supplement 2.2 Humidity units

Humidity unit	Equation
Water vapour pressure: partial pressure of the water vapour in hPa	e
Relative humidity: ratio of the water vapour pressure and the water vapor pressure at saturation in %	$R = (e/E) 100\%$
Dew point τ : temperature, at which the water vapour pressure for saturation can be reached in °C	$E(\tau)$
Water vapour pressure for saturation in with Tetens' equation over water (Stull 2000)	$E = 6.11 e^{\frac{17.6294(T-273.16\text{K})}{T-35.86\text{K}}}$
Water vapour pressure for saturation with Magnus's equation (-45–60 °C over water) according to Sonntag (1990) in hPa	$E = 6.112 e^{\frac{17.624}{253.12+T}}$
Water vapour pressure for saturation with Magnus's equation (-65–0.01 °C over ice) according to Sonntag (1990) in hPa	$E = 6.112 e^{\frac{22.467}{272.62+T}}$
Absolute humidity: mass water vapour per volume moist air in kg m^{-3}	$a = \frac{0.21667 e}{T}$
Specific humidity: mass water vapour per mass moist air in kg kg^{-1} , can be replaced with sufficient accuracy by the mixing ratio or visa versa	$q = 0.622 \frac{e}{p-0.378 e}$
Mixing ratio: mass water vapour per mass dry air in kg kg^{-1}	$m = 0.622 \frac{e}{p-e}$

2.3.2 Integration of the Profile Equation—Roughness and Zero-Plane Displacement

The integration of the profile equation for the momentum flux Eq. (2.48) from height z_0 up to height z is

$$u(z) - u(z_0) = \frac{u_*}{\kappa} \ln \frac{z}{z_0}, \quad (2.60)$$

where z_0 is the height of the extrapolated logarithmic wind profile where $u(z_0) = 0$ as illustrated in Fig. 2.6. Thus, z_0 is simply an integration constant. Because this parameter depends on the characteristics of the surface it is called roughness length, roughness parameter, or roughness height. It varies from 10^{-3} to 10^{-6} m for water and ice, 10^{-2} m for grassland, and up to 0.2 m for small trees. More values are given in Table 2.7.

For neutral conditions, the roughness length z_0 can be determined by extrapolating the wind profile according to Fig. 2.6 to the point $u(z_0) = 0$. This method is limited to roughness elements of small vertical extension (at a maximum forests or settlements with low houses). For more details see Sect. 3.1.1.

For water surfaces, the roughness length z_0 is generally parameterized as a function of the friction velocity. The parameterization by Charnock (1955)

$$z_0 = \frac{u_*^2}{81.1 g} \quad (2.61)$$

Fig. 2.6 Determination of the roughness length z_0 by extrapolation of the log-linear wind profile to the point $u(z_0) = 0$

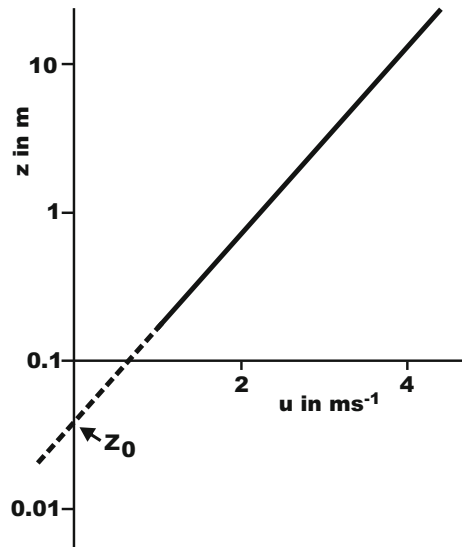


Table 2.7 Roughness length in m from different sources (Reithmaier et al. 2006, updated)

Surface	ESDU (1972)	Troen and Lundtang Petersen (1989)	Wieringa (1992)	Fiedler according to Hasager and Jensen (1999)	Davenport et al. (2000)
Ice	10^{-5}				
Water	$10^{-4} - 10^{-3}$				
Snow	0.002				
Bare soil		0.03	0.004	0.03	0.005
Grassland	0.005–0.02	0.03	0.06	0.08	0.03
Winter crops (winter)		0.1	0.09	0.12	0.1
Winter crops	0.05	0.1	0.18	0.09	0.25
Summer crops	0.05	0.1	0.18	0.09	0.25
Clearings		0.1	0.35	0.004	0.2
Shrubs	0.2	0.4	0.45	0.3	0.5
Conifer forest	1–2	0.4	1.6	0.9	1.0
Deciduous forest	1–2	0.4	1.7	1.2	2.0
Settlement	0.5–2	0.4	0.7	0.5	2.0

is often used in models. However, Eq. (2.61) underestimates z_0 , for low wind velocities, because under these circumstances existing capillary waves are very rough. It is highly recommended to use the relation by Zilitinkevich (1969), which is a combination of Eq. (2.61) and the relation by Roll (1948) in the form

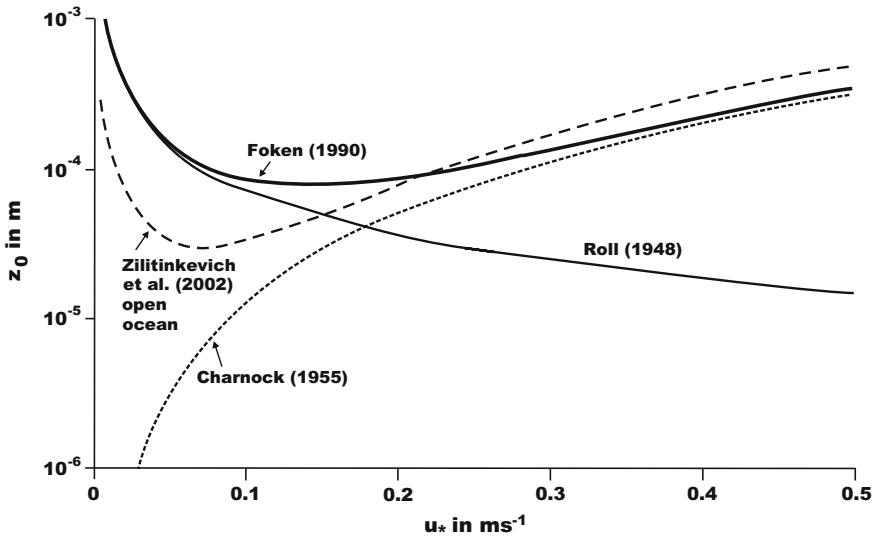
$$z_0 = c_1 \frac{v}{u_*} + \frac{u_*^2}{c_2 g}, \quad (2.62)$$

where the coefficients, c_1 and c_2 are given in Table 2.8 and plotted in Fig. 2.7. For high friction velocities, the data given by Zilitinkevich et al. (2002) show slightly higher roughness-length values in the coastal zone than for the open sea. Because of the remarkable scatter of experimental data for the determination of the roughness length (Kitajgorodskij and Volkov 1965), all combinations of both parameterizations as well the Roll-type for $u_* < 0.1 \text{ m s}^{-1}$ and the Charnock-type for $u_* > 0.1 \text{ m s}^{-1}$ are applicable.

The integration of the equations for the sensible and the latent heat flux is formally identical to those of the momentum flux (Eq. 2.60). The integration constants are the so-called roughness length for temperature and roughness length for humidity. At these heights, the temperature and the humidity are assumed to

Table 2.8 Coefficients for Eq. (2.62)

Author	c_1	c_2
Roll (1948)	0.48	∞
Charnock (1955)	0.0	81.1
Zilitinkevich (1969)	0.1	20.8
Brocks and Krügermeier (1970)	0.0	28.5
Foken (1990)	0.48	81.1
Beljaars (1995)	0.11	55.6
Zilitinkevich et al. (2002)	0.1	56 open ocean 32 coastal zone

**Fig. 2.7** Dependence of the roughness length over water on the friction velocity according to different authors

have approximately the same values as at the ground surface. That this cannot be true was already shown in Fig. 1.5, because near the surface large temperature gradients occur. Therefore, the roughness lengths for scalars cannot be precisely determined. Typically, their values are assumed to be equal to 10% of the roughness length z_0 for momentum.

For atmospheric models these roughness lengths are parameterized (see Sect. 5.3) and used in the following equations

$$T(z) - T(z_{0T}) = \frac{\text{Pr}_t T_*}{\kappa} \ln \frac{z}{z_{0T}}, \quad (2.63)$$

$$q(z) - q(z_{0q}) = \frac{Sc_t q_*}{\kappa} \ln \frac{z}{z_{0q}}, \tag{2.64}$$

where

$$T_* = - \frac{\overline{w'T'}}{u_*} \tag{2.65}$$

is the temperature scale or friction temperature and

$$q_* = - \frac{\overline{w'q'}}{u_*} \tag{2.66}$$

is the humidity scale.

For dense vegetation (grass, grain), the canopy can be considered as a porous medium. The zero-level for the wind field according to Eq. (2.60) is no longer at the ground surface but at a distance d above the surface within the plant canopy. At this level, often called displacement height or zero-plane displacement height d , all equations given thus far are valid analogues to the case of bare soil (Paeschke 1937). The length scale, which is based on this level, is called the aerodynamic scale with $z'(d) = 0$. In contrast, the geometric scale, which is measured from the ground surface, is $z = z' + d$ (Fig. 2.8). Because Eq. (2.60) is valid only for the aerodynamic scale, the expression for low vegetation using the geometric scale as reference gives:

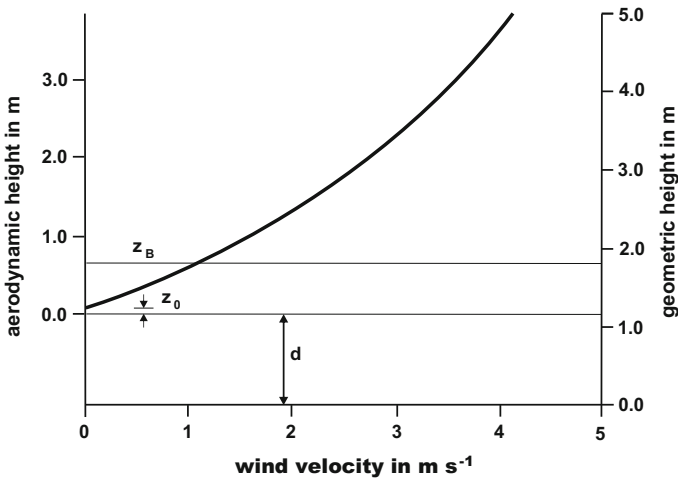


Fig. 2.8 Aerodynamic and geometric scale for dense vegetation ($d = 1.2$ m)

$$u(z) = \frac{u_*}{\kappa} \ln \frac{z-d}{z_0} \quad (2.67)$$

Consequently, all profile equations and equations for integral turbulence characteristics, which are used in this and the following chapters, must be modified for low vegetation by replacing “ z ” with “ $z-d$ ”. The roughness length z_0 in Eq. (2.67) is related to the new aerodynamic zero-level and Table 2.7 can be applied. Sometimes in the literature the denominator is given as $z_0 - d$. In this case z_0 is measured from the ground. High vegetation (forest) and tall buildings require special considerations (see Sect. 3.1.2).

The log-linear extrapolated plot of the wind profile above a dense plant canopy with the geometric height as the ordinate cuts the ordinate at $u(z_0 + d) = 0$. Thus, it is not possible to determine the roughness and displacement heights in a simple way. Instead, a system of equations must be solved. However, it is possible to use a value of z_0 from Table 2.7 and then calculate d . A simple approximation is also given by

$$z_0 = 0.1 z_B, \quad (2.68)$$

where z_B is the canopy height. Another method is to assume that the displacement height is about 2/3 of the canopy height. Therefore, with a known value of $z_0 + d$ the roughness length can be determined by:

$$z_0 = [z_0 + d] - \frac{2}{3} z_B \quad (2.69)$$

The determination of the zero-plane displacement for heterogeneous surfaces, high vegetation and buildings is discussed in Sect. 3.1.2.

2.3.3 Monin-Obukhov's Similarity Theory

The equations given in Sect. 2.3.1 are strictly speaking only valid in the dynamic sub-layer in which the influence of thermal stratification can be neglected. Monin and Obukhov (1954) used dimensional analysis according to Buckingham's Π -theorem (Supplement 2.3), to extend these equations to the non-neutral (diabatic) case (Foken 2006a). In this analysis, the dependent parameters in the surface layer are the height z in m, the friction velocity u_* in m s^{-1} , the kinematic heat flux

$$\overline{w'T'} = \frac{Q_H}{\rho c_p} \quad (2.70)$$

in K m s^{-1} , and the buoyancy parameter g/T in $\text{m s}^{-2} \text{K}^{-1}$. The independent dimensions are the length in meters, the time in seconds, and the temperature in K

degrees. The dimensionless parameter that characterizes the processes in the surface layer is (also called Obukhov number or Obukhov stability parameter)

$$\zeta = z/L, \quad (2.71)$$

where

$$L = - \frac{u_*^3}{\kappa \frac{g}{T} \frac{Q_H}{\rho c_p}}. \quad (2.72)$$

Supplement 2.3 Buckingham's Π -theorem

Buckingham's Π -theorem (Buckingham 1914; Kantha and Clayson 2000) states that for $n + 1$ dependent parameters and k independent dimensions, there exist exactly $n + 1 - k$ dimensionless parameters which characterize the process. This can be demonstrated for the free throw of an object (Kitajgorodskij 1976), where z , u_0 , g and x are the $n + 1$ dependent parameters corresponding to the dropping height, velocity of the throw, gravity acceleration, and distance of the impact point. The independent dimensions are the length in m and the time in s. The benefit of the dimension analysis is shown stepwise:

- The determination of $x = f(z, u_0, g)$ from many single experiments is very expensive.
- The assumption $g = \text{const}$ gives an array of curves for different dropping heights.
- Using Buckingham's Π -theorem one can determine both dimensionless values $x^+ = x/z$ and $z^+ = g z u_0^2$, which gives a direct functional relation between x^+ and z^+ .
- If you increase the number of dimensions by separation of the length scale for the horizontal and vertical direction, the process can be described with only one dimensionless parameter $x^* = c u_0 (z g^{-1})^{1/2}$. With some experiments it is even possible to determine for the constant c the standard deviation.

The difficulty in the application of Buckingham's Π -theorem is the selection of the parameters, the dimensions, and the determination of the suitable dimensionless parameters. Because of the many influencing parameters in meteorology, this theorem is very important.

The characteristic length scale L is called the Obukhov length (Obukhov 1946). Initially, the notation Monin-Obukhov-length was used, but this is, in the historical sense, not exact (Businger and Yaglom 1971). The Obukhov length gives a relation

between dynamic, thermal, and buoyancy processes, and is proportional to the height of the dynamic sub-layer (Obukhov 1946), but is not identical with it (Monin and Yaglom 1973, 1975).

Currently (Stull 1988), the Obukhov length is derived from the TKE-equation Eq. (2.42). A physical interpretation of L was made by Bernhardt (1995), i.e., the absolute value of the Obukhov length is equal to the height of an air column in which the production ($L < 0$) or the loss ($L > 0$) of TKE by buoyancy forces is equal to the dynamic production of TKE per volume unit at any height z multiplied by z .

It is more accurate to define the Obukhov length using the potential temperature. Furthermore, for buoyancy considerations the content of water vapour is important, which changes the air density. Therefore, virtual potential temperature θ_v should be applied. The Obukhov length is then defined as:

$$L = - \frac{u_*^3}{\kappa \frac{\rho}{\theta_v} w' \theta'_v} \quad (2.73)$$

This is precise, but is not often used because the universal functions, discussed below, were determined in the lower surface layer and often in dry regions. Observations made in other regions showed within the accuracy of the measurements no significant differences.

The application of Monin-Obukhov similarity theory on the profile equations Eqs. (2.46)–(2.48) is done using the so-called universal functions $\varphi_m(\zeta)$, $\varphi_H(\zeta)$ and $\varphi_E(\zeta)$ for the momentum, sensible and latent heat exchange respectively. Therefore, a new functional dependence on the dimensionless parameter ζ , is given along with Eqs. (2.51) and (2.54):

$$u_* = \sqrt{-\overline{u'w'}} = \frac{\kappa z}{\varphi_m(\zeta)} \frac{\partial u}{\partial z} = \frac{\kappa}{\varphi_m(\zeta)} \frac{\partial u}{\partial \ln z} \quad (2.74)$$

$$\frac{\overline{w'T'}}{u_*} = - \frac{\kappa / \text{Pr}_t}{\varphi_H(\zeta)} \frac{\partial T}{\partial \ln z} \quad (2.75)$$

$$\frac{\overline{w'q'}}{u_*} = - \frac{\kappa / \text{Sc}_t}{\varphi_E(\zeta)} \frac{\partial q}{\partial \ln z} \quad (2.76)$$

The universal functions account for the effects of stronger mixing in the unstable case, which leads to a decrease of the gradient and an increase of the flux. In the stable case the opposite conditions apply. The universal functions can be approximated by a Taylor series (Monin and Obukhov 1954) with the argument ζ :

$$\varphi(\zeta) = 1 + \beta_1 \zeta + \beta_2 \zeta^2 + \dots \quad (2.77)$$

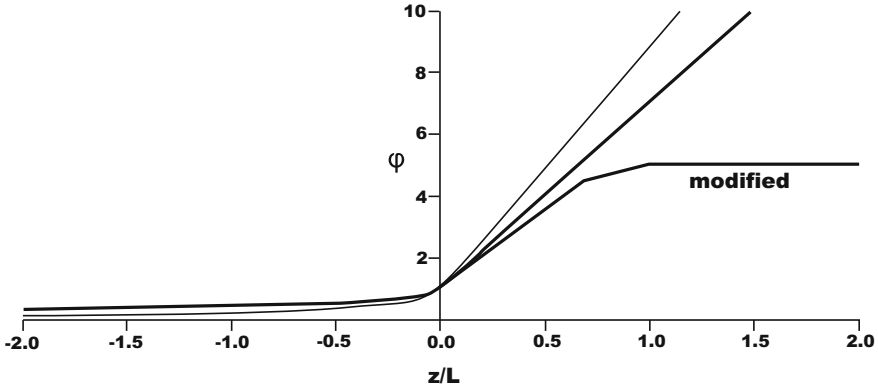


Fig. 2.9 Typical graph of the universal functions for momentum flux (*bold line*) and sensible and latent heat flux (*fine line*); ‘modified’ indicates the function is characterized under the conditions of *z-less*-scaling

Based on Obukhov’s (1946) investigations, the so-called O’KEYPS-function (Kaimal, Elliot, Yamamoto, Panofsky, Sellers) followed from the studies made in the 1950s and 60s (Panofsky 1963; Businger and Yaglom 1971; Businger 1988):

$$[\varphi_m(\zeta)]^4 - \gamma_1 \cdot \zeta \cdot [\varphi_m(\zeta)]^3 = 1 \tag{2.78}$$

According to Businger et al. (1971) it follows that $\gamma_1 \approx 9$ ($-2 < \zeta < 0$) and that the form $\varphi_m(\zeta) \cong (-\gamma_1 \zeta)^{-1/3}$ fulfills the O’KEYPS-equation which applies to the conditions of free convection. The currently used form of the universal functions (Fig. 2.9) is numerically only slightly different (Kramm and Herbert 2009):

$$\varphi_m(\zeta) = (1 + \gamma_2 \cdot \zeta)^{-1/4}, \tag{2.79}$$

which is called the Businger-Dyer-Pandolfo-relationship (Pandolfo 1966; Businger 1988).

The relationships between the universal functions for momentum and sensible heat are given by:

$$\begin{aligned} \varphi_H &\approx \varphi_m^2 && \text{for } \zeta < 0 \\ \varphi_H &\approx \varphi_m && \text{for } \zeta \geq 0 \end{aligned} \tag{2.80}$$

Consequently, the influence of stratification in the surface layer on the universal functions can be described with the stability parameter ζ . The universal functions are generally defined in the range of $-1 < \zeta < 1$. In the stable case ($\zeta > 1$) a height-independent scaling occurs, the so-called *z-less* scaling (Wyngaard 1973). In this case, the eddy sizes do not depend on the height above the ground surface but on the local Obukhov-length (Table 2.9, Fig. 2.9).

Table 2.9 Determination of the stratification in the surface layer dependent on the dimensionless parameter ζ and the universal function $\varphi(\zeta)$

Stratification	Remark	ζ	$\varphi(\zeta)$
Unstable	Free convection, independent from u_*	$-1 > \zeta$	No definition
	Dependent from u_* , T_*	$-1 < \zeta < 0$	$\varphi(\zeta) < 1$
Neutral	Dependent from u_*	$\zeta \sim 0$	$\varphi(\zeta) = 1$
Stable	Dependent from u_* , T_*	$0 < \zeta < 0.5 \dots 2$	$1 < \varphi(\zeta) < 3 \dots 5$
	Independent from z	$0.5 \dots 1 < \zeta$	$\varphi(\zeta) \sim \text{const} \sim 4 \dots 7$

Table 2.10 Universal function according to Businger et al. (1971), recalculated by Höögström (1988)

Stratification	$\varphi_m(\zeta)$	$\varphi_H(\zeta) \sim \varphi_E(\zeta)$, $Pr_t = Sc_t = 1$
Unstable	$(1 - 19.3 \zeta)^{-1/4}$	$0.95 (1 - 11.6 \zeta)^{-1/2}$
Stable	$1 + 6.0 \zeta$	$0.95 + 7.8 \zeta$

Presently the universal functions derived from the Kansas-experiment of 1968 by Businger et al. (1971) and later modified by Höögström (1988) are widely used. Höögström (1988) considered important criticisms of the Kansas-experiment, for example of the wind measurements (Wieringa 1980), and has re-calculated the von-Kármán constant from $\kappa = 0.35$ to the presently used value of $\kappa = 0.40$ (Table 2.10).

The universal functions given in Table 2.10 are recommended for use. In the last 40 years, many universal functions were determined. The most important of these are given in Appendix A.4. A difficulty in applying the universal functions is the normalization. The basics were discussed by Yaglom (1977). For applying the universal functions, one must consider if the turbulent Prandtl number is part of the universal function, is used in the profile equation, or even included in the Obukhov length (Skeib 1980). Furthermore, all universal functions must be recalculated for the updated value of the von-Kármán constant of 0.4 (Höögström 1988). It must be noted that the universal functions by Zilitinkevich and Tschalikov (1968) and Dyer (1974) are widely used in the Russian and English literature respectively. Also interesting, is the universal function by Skeib (1980) which is based on the separation of the atmospheric boundary layer into a dynamical sub-layer (without influence of stratification) and a surface layer. In analogy with hydrodynamics, critical values for the separation of both layers are used. A disadvantage is the non-continuous function, but the integration gives a physically rational function.

There are only a few papers with results using the universal function for the water vapor exchange. Therefore, the universal function for the sensible heat flux is

Table 2.11 The von-Kármán constant according to different authors (Foken 1990, 2006), where the value by Högström (1996) is recommended

Author	κ
Monin and Obukhov (1954)	0.43
Businger et al. (1971)	0.35
Pruitt et al. (1973)	0.42
Högström (1974)	0.35
Yaglom (1977)	0.40
Kondo and Sato (1982)	0.39
Högström (1985, 1996)	0.40 ± 0.01
Andreas et al. (2004)	0.387 ± 0.004

used widely for the latent heat flux and the fluxes of trace gases with accordingly identical numbers for the turbulent Prandtl and Schmidt number.

Applying the universal function in the stable case is difficult. It is already well known that the universal function in the above form underestimates the turbulent exchange process. The assumption of a nearly constant universal function, which also supports the z -less scaling is obvious. The lack of measurements has not allowed a general applied formulation (Andreas 2002). Handorf et al. (1999) based on measurements in Antarctica that for $\zeta > 0.6$ the universal function becomes constant $\varphi_m \sim 4$. Cheng and Bruntseart (2005) found for $\zeta > 0,6$ a value of $\varphi_m \sim 7$ for the CASES-99-experiment.

The uncertainty of the universal functions is similar to those of the turbulent Prandtl number (Table 2.6), and is also dependent on the accuracy of the measurement methods. Furthermore, the determination of Pr_t and κ for neutral conditions is relevant for the universal function at $\zeta = 0$. The von-Kármán constant is presently accepted as $\kappa = 0.40 \pm 0.01$ (Högström 1996). But a slight dependency on the Rossby and Reynolds numbers was discovered (Onceley et al. 1996), which is probably a self-correlation effect (Andreas et al. 2004). An overview of values of the von-Kármán constant appearing in the literature is shown in Table 2.11. Regarding the universal function, the following accuracies are given by Högström (1996), where normally the virtual temperature is not applied:

$$\begin{aligned}
 |z/L| \leq 0.5: & \quad |\delta\varphi_H| \leq 10 \% \\
 |z/L| \leq 0.5: & \quad |\delta\varphi_m| \leq 20 \% \\
 z/L > 0.5: & \quad \varphi_m, \varphi_H = \text{const} ?
 \end{aligned}
 \tag{2.81}$$

The discussion of the accuracy of the parameters and functions is still ongoing. For example, a dependence on the mixed layer height cannot be excluded (Johansson et al. 2001). This means that processes in the surface layer may be influenced non-locally by the whole boundary layer.

In addition to the Obukhov number ζ , the Richardson number Eq. (2.20) is used to determine atmospheric stability. The definitions of the gradient, bulk, and flux Richardson numbers are:

Gradient Richardson number:

$$Ri = -\frac{g}{T} \cdot \frac{\partial T / \partial z}{(\partial u / \partial z)^2} \quad (2.82)$$

Bulk Richardson number:

$$Ri_B = -\frac{g}{T} \frac{\Delta T \Delta z}{(\Delta u)^2} \quad (2.83)$$

Flux Richardson number:

$$Rf = \frac{g}{T} \frac{\overline{w'T'}}{\overline{w'u'}(\partial u / \partial z)} \quad (2.84)$$

Analogous to the Obukhov length, the temperature can be replaced by the virtual potential temperature.

The critical Richardson numbers are $Ri_c = 0.2$ and $Rf_c = 1.0$, for which in the case of stable stratification the turbulent flow changes suddenly to a quasi laminar, non-turbulent, flow or turbulence becomes intermittent. The conversion of ζ into Ri is stratification-dependent according to the relations (Businger et al. 1971; Arya 2001):

$$\begin{aligned} \zeta &= Ri & \text{for } Ri < 0 \\ \zeta &= \frac{Ri}{1-5Ri} & \text{for } 0 \leq Ri \leq 0.2 = Ri_c \end{aligned} \quad (2.85)$$

An overview about the ranges of different stability parameters is shown Table 2.12.

The integration of the profile Eqs. (2.74)–(2.76) using the universal functions in the form of Eq. (2.79) for the unstable case is not trivial and was first presented by Paulson (1970). For the wind profile, the integration from z_0 to z using the definition of the roughness length $u(z_0) = 0$ is

$$u(z) - u(z_0) = u(z) = \frac{u_*}{\kappa} \left[\ln \frac{z}{z_0} - \int \varphi_m(\zeta) d\zeta \right], \quad (2.86)$$

$$u(z) = \frac{u_*}{\kappa} \left[\ln \frac{z}{z_0} - \psi_m(\zeta) \right], \quad (2.87)$$

Table 2.12 Overview about different stability parameters

Stratification	Temperature	Ri	L	$\zeta = z/L$
Unstable	$T(0) > T(z)$	< 0	< 0	< 0
Neutral	$T(0) \sim T(z)$	~ 0	$\pm \infty$	~ 0
Stable	$T(0) < T(z)$	$0 < Ri < 0.2 = Ri_c$	> 0	$0 < \zeta < \sim 1$

where the integral of the universal function, $\psi_m(\zeta)$, is:

$$\psi_m(\zeta) = \int_{z_0/L}^{z/L} [1 - \varphi_m(\zeta)] \frac{d\zeta}{\zeta} \quad (2.88)$$

Accordingly, it follows for the integrated version for the sensible heat flux, which can also be applied for other scalars:

$$T(z) - T(z_{0T}) = \frac{\text{Pr}_r T_*}{\kappa} \left[\ln \frac{z}{z_{0T}} - \int \varphi_h(\zeta) d\zeta \right] \quad (2.89)$$

$$T(z) - T(z_{0T}) = \frac{\text{Pr}_r T_*}{\kappa} \left[\ln \frac{z}{z_{0T}} - \psi_h(\zeta) \right] \quad (2.90)$$

$$\psi_h(\zeta) = \int_{z_{0T}/L}^{z/L} [1 - \varphi_h(\zeta)] \frac{d\zeta}{\zeta} \quad (2.91)$$

The integration of the universal function for the momentum and sensible heat flux for unstable conditions according to Businger et al. (1971) in the form of Högström (1988) is

$$\psi_m(\zeta) = \ln \left[\left(\frac{1+x^2}{2} \right) \left(\frac{1+x}{2} \right)^2 \right] - 2 \tan^{-1} x + \frac{\pi}{2} \quad \text{for } \frac{z}{L} < 0, \quad (2.92)$$

$$\psi_h(\zeta) = 2 \ln \left(\frac{1+y}{2} \right) \quad \text{for } \frac{z}{L} < 0, \quad (2.93)$$

with

$$x = (1 - 19.3\zeta)^{1/4} \quad y = 0.95(1 - 11.6\zeta)^{1/2}. \quad (2.94)$$

It is obvious that the cyclic term in Eq. (2.92) is not physically realistic. But this term is relatively small and has no remarkable influence on the result. In the stable case there are very simple solutions for the integrals of the universal functions:

$$\psi_m(\zeta) = -6 \frac{z}{L} \quad \text{for } \frac{z}{L} \geq 0 \quad (2.95)$$

$$\psi_h(\zeta) = -7.8 \frac{z}{L} \quad \text{for } \frac{z}{L} \geq 0 \quad (2.96)$$

The universal function according to the Businger-Dyer-Pandolfo relation Eq. (2.79) shows a good asymptotic behaviour for neutral stratification. A further version for the integration was proposed by Berkowicz and Prahm (1984).

2.3.4 Bowen-Ratio Similarity

The Bowen ratio (Bowen 1926) is defined as the ratio of the sensible to the latent heat flux:

$$Bo = \frac{Q_H}{Q_E} \quad (2.97)$$

Using Eqs. (2.75) and (2.76), and taking the conversion between kinematic and energetic units into consideration according to Eqs. (2.58) and (2.59) a very simple relation develops. With the assumption $\varphi_H(\zeta) \sim \varphi_E(\zeta)$, for neutral stratification or restriction to the dynamic sub-layer, $Pr_t \sim Sc_t$, and replacing the partial derivatives by finite-differences gives

$$Bo = \frac{c_p}{\lambda} \frac{\Delta T}{\Delta q} = \frac{c_p}{\lambda} \frac{p}{0.622} \frac{\Delta T}{\Delta e} = \gamma \frac{\Delta T}{\Delta e}, \quad (2.98)$$

where the psychrometric constant is $\gamma = 0.667 \text{ hPa K}^{-1}$ for $p = 1013.25 \text{ hPa}$ and $T = 20 \text{ }^\circ\text{C}$.

A special case of the flux-gradient similarity Eq. (2.98), is the so-called Bowen-ratio similarity. The ratio of the gradients of temperature and humidity between two heights behaves like the Bowen ratio. This simplification is the basis of the Bowen-ratio method (see Sect. 4.1.1). It must be noted that the simplifications used are also limitations of the method.

The generalization of this similarity is

$$\frac{F_x}{F_y} \approx \frac{\Delta x}{\Delta y}, \quad (2.99)$$

i.e., the ratio of two fluxes is proportional to the ratio of the differences of the relevant state parameters between two heights.

This equation opens the possibility of determining the flux of an inert gas if the energy flux is known, if the differences of the trace gas concentrations can be determined with a high accuracy, and if the above made simplifications can be accepted. This method was proposed as a modified Bowen-ratio method by Businger (1986), compare with Sect. 4.1.1.

2.4 Flux-Variance Similarity

Analogous to the derivation of the *TKE* equation, Eq. (2.42), the balance equations for the momentum and sensible heat flux can be derived (Wyngaard et al. 1971a; Foken et al. 1991):

$$\frac{\partial \overline{w'u'}}{\partial t} = \underbrace{-\overline{w'^2} \frac{\partial \bar{u}}{\partial z}}_{\text{II}} - \frac{g}{T} (\overline{u'T'}) - \frac{\partial}{\partial z} \overline{u'w'^2} - \frac{1}{\rho} \frac{\partial (\overline{w'p'})}{\partial z} - \varepsilon \quad \text{VII} \quad (2.100)$$

$$\frac{\partial \overline{w'T'}}{\partial t} = \underbrace{-\overline{w'^2} \frac{\partial \bar{T}}{\partial z}}_{\text{III}} - \frac{g}{T} (\overline{T'^2}) - \frac{\partial}{\partial z} \overline{T'w'^2} - \frac{1}{\rho} \frac{\partial (\overline{T'p'})}{\partial z} - N_T \quad \text{VII} \quad (2.101)$$

These equations include the standard deviations of the vertical wind component and the temperature:

$$\sigma_w = \sqrt{\overline{w'^2}} \quad \text{und} \quad \sigma_T = \sqrt{\overline{T'^2}} \quad (2.102)$$

For steady state conditions and after estimation of the magnitude of the terms II and VII in Eq. (2.100) and terms III and VII in Eq. (2.101) it follows for the surface layer (Wyngaard et al. 1971a; Foken et al. 1991):

$$\sigma_w/u_* \cong \text{const.} \quad \text{und} \quad \sigma_T/T_* \cong \text{const.} \quad (2.103)$$

These normalized standard deviations are also called integral turbulence characteristics (Tillman 1972), because they integrally characterize the state of turbulence over all frequencies. For the integral turbulence characteristics of the three wind components, the following values are given (Lumley and Panofsky 1964; Panofsky and Dutton 1984):

$$\begin{aligned} \sigma_w/u_* &\cong 1.25 \\ \sigma_u/u_* &\cong 2.45 \\ \sigma_v/u_* &\cong 1.9 \end{aligned} \quad (2.104)$$

The constancy is only valid for neutral stratification. From similarity relations for diabatic conditions it follows (Foken et al. 1991):

$$\sigma_w/u_* = a[\varphi_m(z/L)]^{-0.5} \quad (2.105)$$

$$\sigma_T/T_* = b \left[\frac{z}{L} \varphi_h(z/L) \right]^{-0.5} \quad (2.106)$$

Many dependencies are reported in the literature for the integral turbulence characteristics under diabatic conditions (see Appendix A.4). Therefore, for the integral turbulence characteristics a general form is used for the wind components

$$\sigma_{u,v,w}/u_* = c_1(z/L)^{c_2}, \quad (2.107)$$

and for temperature and other scalars

$$\sigma_T/T_* = c_1(z/L)^{c_2}, \quad (2.108)$$

where $c_2 = -1/3$ is often applied (Wyngaard 1973). At least for the vertical wind, there are no significant differences between the available parameterizations. The most common parameterization by Panofsky et al. (1977) can be applied in the neutral and unstable case too:

$$\sigma_w/u_* = 1.3 \left(1 - 2 \frac{z}{L}\right)^{1/3} \quad (2.109)$$

Based on these findings, the experimentally verified relationships are given in Table 2.13.

The integral turbulence characteristics for temperature and other scalars in the case of neutral stratification are not exact because $T_* \rightarrow 0$. In the case of unstable stratification for wind components and scalars, dependencies on stratification were found. Thus, some authors (Panofsky et al. 1977; Peltier et al. 1996; Johansson et al. 2001) reported a dependency on the mixed layer height in the case of strong unstable stratification. But the difference is relevant only for free convection (Thomas and Foken 2002). For stable stratification, only a few verified measurements are available. Therefore, the use of the given parameterizations for the unstable case with the argument $|(z - d)/L|$ is recommended as a first approximation. For temperature, a slightly modified approach is given in Table 2.13 (Thomas and Foken 2002).

Based on Rossby similarity (Garratt 1992, see Sect. 2.6.2) some authors (Yaglom 1979; Tennekes 1982; Högström 1990; Smedman 1991) assumed, at least in the neutral case, a visible dependency on the Coriolis parameter. The verification

Table 2.13 Integral turbulence characteristics for diabatic stratification (Foken et al. 1991, 1997; Thomas and Foken 2002)

Parameter	z/L	c_1	c_2
σ_w/u_*	$0 > z/L > -0.032$	1.3	0
	$-0.032 > z/L$	2.0	1/8
$\sigma_{i'}/u_*$	$0 > z/L > -0.032$	2.7	0
	$-0.032 > z/L$	4.15	1/8
σ_T/T_*	$0.02 < z/L < 1$	1.4	-1/4
	$0.02 > z/L > -0.062$	0.5	-1/2
	$-0.062 > z/L > -1$	1.0	-1/4
	$-1 > z/L$	1.0	-1/3

Table 2.14 Parameterization of the integral turbulence characteristics for neutral and slightly unstable and stable stratification (Thomas and Foken 2002)

Parameter	$-0,2 < z/L < 0,4$
σ_w/u_*	$0.21 \ln\left(\frac{z+f}{u_*}\right) + 3.1 \quad z_+ = 1 \text{ m}$
σ_u/u_*	$0.44 \ln\left(\frac{z+f}{u_*}\right) + 6.3 \quad z_+ = 1 \text{ m}$

was developed by Högström et al. (2002). A parameterization according to this finding for the neutral and slightly unstable and stable range is given in Table 2.14. For scalars, such a parameterization cannot be found due to the high dependency on the stratification in this range.

2.5 Turbulence Spectrum

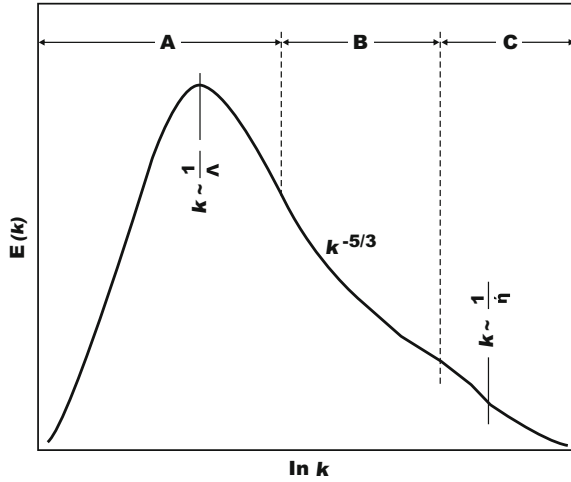
Knowledge of the turbulence spectrum (see Sect. 1.4.3) is critically important for choosing sensors and defining optimal sensing strategies for given atmospheric conditions. Many sensing and also modelling techniques are possible only within certain portions of the turbulence spectrum, or are based on assumptions about the distribution of spectral energy density. Turbulence spectra vary depending on the state parameters, fluxes, and micrometeorological conditions. In the frequency range of interest to micrometeorology, i.e. periods shorter than about 30 min, three ranges can be identified. The range of production of the turbulent energy by the mean flow is characterized by the integral turbulent length scale Λ , which is in the order of 10–500 m (Kaimal and Finnigan 1994). The typical frequency range is $f \sim 10^{-4}$ Hz (note that here f is not the Coriolis parameter). This range is followed by the inertial sub-range in which turbulence is assumed to be isotropic, i.e. the turbulent movements have no preferential direction. In this range, a well defined energy decrease with increasing frequency occurs according to Kolmogorov's laws (Kolmogorov 1941a, b). The decrease of energy is proportional to $f^{-5/3}$. After multiplying the energy by the frequency the Kolmogorov laws predict an $f^{-2/3}$ decrease for state parameters and an $f^{-4/3}$ decrease for the fluxes. In the third range, with frequencies of 10–30 Hz the kinetic energy of the small eddies is transformed into thermal energy (energy dissipation). The typical dissipation length scale is the Kolmogorov's microscale

$$\eta = \left(\frac{\nu^3}{\varepsilon}\right)^{1/4}, \quad (2.110)$$

which is about 10^{-3} m.

The three parts of the turbulence spectrum in the micrometeorological range are plotted against wave number in Fig. 2.10. Maximum energy occurs at the integral turbulence length $\sim 1/k$. Note that $\Lambda = \pi/k$, is the Eulerian integral turbulence

Fig. 2.10 Schematic plot of the turbulence spectra and the ranges of energy production (A), the inertial sub-range (B) and the dissipation range (C) dependent on the wave number k (Adapted from Kaimal and Finnigan 1994, with kind permission of © Oxford University Press, Oxford 1994, All rights reserved)



length scale. This length scale can be given for all wind components and scalars. According to Taylor's frozen turbulence hypothesis (Taylor 1938), wave number and frequency are related as:

$$k = 2\pi f / \bar{u} \quad (2.111)$$

Using Eq. (2.111), the integral turbulence length scale can be transferred into an integral turbulence time scale T_u which is defined by the autocorrelation function ρ_u for the horizontal velocity perturbation (Monin and Yaglom 1973; 1975; Schlichting and Gersten 2003; Wyngaard 2010),

$$\Lambda_u = \bar{u} \cdot T_u = \bar{u} \int_0^{\infty} \rho_u(\xi) d\xi = \bar{u} \int_0^{\infty} \frac{\overline{u'(t) u'(t + \xi)}}{\sigma_u^2} d\xi. \quad (2.112)$$

Because the autocorrelation function is usually an exponential function, the integral time scale, τ , is given $\rho(\tau) = 1/e \sim 0.37$. This is schematically illustrated in Fig. 2.11.

The energy spectrum under the assumption of local isotropy along with the Kolmogorov constant $\beta_u \sim 0.5-0.6$ (Kolmogorov 1941b) can be given in the inertial sub-range by the so-called $-5/3$ -law, here presented for the horizontal wind component:

$$E_u(k) = \beta_u \varepsilon^{2/3} k^{-5/3} \quad (2.113)$$

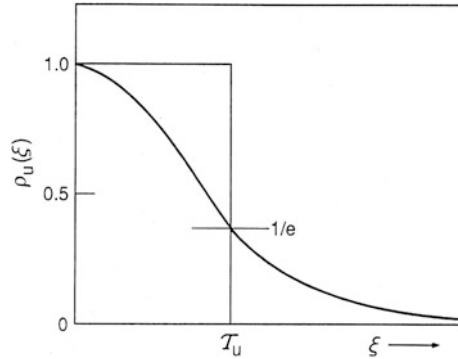


Fig. 2.11 Autocorrelation function and its relation to the integral time scale. The value $1/e$ is a good approximation for which the area of the shown rectangle is equal to the area below the exponential plot (Adapted from Kaimal and Finnigan 1994, with kind permission of © Oxford University Press, Oxford 1994, All rights reserved)

In an analogous way, the energy spectrum of the temperature in the inertial sub-range is

$$E_T(k) = \beta_T N_T \varepsilon^{-1/3} k^{-5/3}, \tag{2.114}$$

with the Kolmogorov constant $\beta_T \sim 0.75\text{--}0.85$ (Corrsin 1951), and N_T is the dissipation rate of the variance of the temperature Eq. (2.94). For humidity, the inertial sub-range spectrum is

$$E_q(k) = \beta_q N_q \varepsilon^{-1/3} k^{-5/3} \tag{2.115}$$

with the Kolmogorov constant $\beta_q \sim 0.8\text{--}1.0$. The mathematical background for spectral diagrams is briefly given in Supplement 2.4.

Supplement 2.4 Fourier series and frequency spectrum

A function f , e.g., a time series of a meteorological parameter with turbulent fluctuations (Fig. 1.13), can be represented by a system of orthogonal functions:

$$f(x) = \frac{a_0}{2} + \sum_{k=1}^{\infty} (a_k \cos kx + b_k \sin kx) \tag{S2.3}$$

$$a_k = \frac{1}{\pi} \int_0^{2\pi} f(x) \cos kx \, dx \quad b_k = \frac{1}{\pi} \int_0^{2\pi} f(x) \sin kx \, dx \tag{S2.4}$$

In an analogous way, its representation by an exponential function is possible:

$$f(x) = \sum_{k=-\infty}^{\infty} (c_k e^{ikx}) \quad c_k = \frac{1}{2\pi} \int_{-\pi}^{\pi} f(x) e^{-ikx} dx \quad (\text{S2.5})$$

The Fourier transformation is an integral transformation, which converts a function of time into a function of frequency:

$$F(\omega) = \frac{1}{\sqrt{2\pi}} \int_{-\infty}^{\infty} f(t) e^{i\omega t} dt \quad (\text{S2.6})$$

The square root of the time integral over the frequency spectrum (energy spectrum, power spectrum) corresponds to the standard derivation. The frequency spectrum of two time series is called the cross spectrum. Its real part is the co-spectrum, and the time integral of the co-spectrum corresponds to the covariance.

Multiplying the TKE equation, Eq. (2.42), by the factor $\kappa z/u_*^3$ and assuming steady state conditions ($\partial\bar{\epsilon}/\partial t = 0$), gives the dimensionless TKE equation for the surface layer (Wyngaard and Coté 1971; Kaimal and Finnigan 1994):

$$\varphi_m - \frac{z}{L} - \varphi_t - \varphi_\epsilon + I = 0 \quad (2.116)$$

The imbalance term I is based on the pressure term. I disappears in the unstable case and is of order z/L in the stable case. The transport term, φ_t , is of order $-z/L$ in the unstable case, and disappears in the stable case. The dimensionless energy dissipation term is

$$\varphi_\epsilon = \frac{\kappa z \epsilon}{u_*^3}, \quad (2.117)$$

which can be described by a universal function (Kaimal and Finnigan 1994):

$$\varphi_\epsilon^{2/3} = \begin{cases} 1 + 0.5|z/L|^{2/3} & \text{for } z/L \leq 0 \\ (1 + 5z/L)^{2/3} & \text{for } z/L \geq 0 \end{cases} \quad (2.118)$$

$$\varphi_\epsilon^{2/3} = \begin{cases} 1 + 0.5|z/L|^{2/3} & \text{for } z/L \leq 0 \\ (1 + 5z/L)^{2/3} & \text{for } z/L \geq 0 \end{cases}$$

Additional universal functions for the energy dissipation are given in Appendix A.4. A practical application of these equations is the determination of the friction velocity using a scintillometer (see Sect. 6.2.5). Also, the energy spectrum of the horizontal wind can be derived in the inertial sub-range (Kaimal and Finnigan 1994):

$$\begin{aligned} \frac{f \cdot S_u(f)}{u_*^2} &= \frac{0.55}{(2\pi)^{2/3}} \left(\frac{\varepsilon^{2/3} z^{2/3}}{u_*^2} \right) \left(\frac{fz}{\bar{u}} \right)^{-2/3} \\ &= \frac{0.55}{(2\pi\kappa)^{2/3}} \phi_\varepsilon^{2/3} \left(\frac{fz}{\bar{u}} \right)^{-2/3} \end{aligned} \tag{2.119}$$

The turbulence spectra of various parameters differ significantly in peak frequency (maximum of the energy density) and their dependence on the stratification. The peak frequency of the vertical wind corresponds to the highest frequencies (0.1–1 Hz), and those of the horizontal wind are one order of magnitude lower (Fig. 2.12). The vertical wind shows this typical form of spectrum for stable (peak frequency shifted to higher frequencies) and unstable stratification. For the other wind components and scalars, the peak frequencies are shifted to lower frequencies,

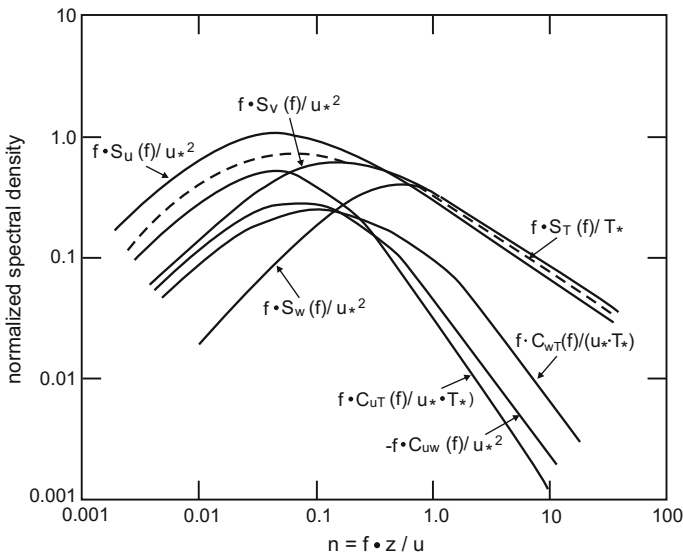


Fig. 2.12 Models of the energy density spectrum of state variables and fluxes (Adapted from Kaimal et al. 1972, with kind permission of © John Wiley & Sons Inc., New York 1972, All rights reserved)

and because of large scatter in the data, they are often not clearly seen. In this range, mixed layer height often becomes an important, additional scaling parameter.

Energy density spectra are often used for the correction of measurement data (see Sect. 4.1.2). Because of the difficulty in calculating spectra, models of spectra are often applied. Such models were parameterized by Kaimal et al. (1972) on the basis of the data of the Kansas experiment. With the usual normalization of the frequency according to Eq. (1.19)

$$n = f \frac{z}{\bar{u}}, \quad (2.120)$$

the wind components for neutral and slightly unstable stratification (Kaimal and Finnigan 1994) are:

$$\frac{f S_u(f)}{u_*^2} = \frac{102 n}{(1 + 33 n)^{5/3}} \quad (2.121)$$

$$\frac{f S_v(f)}{u_*^2} = \frac{17 n}{(1 + 9.5 n)^{5/3}} \quad (2.122)$$

$$\frac{f S_w(f)}{u_*^2} = \frac{2.1 n}{1 + 5.3 n^{5/3}} \quad (2.123)$$

Højstrup (1981) proposed a stability-dependent parameterization for the vertical wind for unstable stratification:

$$\frac{f S_w(f)}{u_*^2} = \frac{2 n}{1 + 5.3 n^{5/3}} + \frac{32 n (z/L - 1)^{2/3}}{(1 + 17 n)^{5/3}} \quad (2.124)$$

For the temperature spectrum, which can also be used for other scalars, Kaimal et al. (1972) published the following parameterization:

$$\frac{f S_T(f)}{T_*^2} = \left\{ \begin{array}{ll} \frac{53.4 n}{(1 + 24 n)^{5/4}} & \text{for } n < 0.5 \\ \frac{24.4 n}{(1 + 12.5 n)^{5/3}} & \text{for } n \geq 0.5 \end{array} \right\} \quad (2.125)$$

For the co-spectra, (Kaimal and Finnigan 1994) proposed for the unstable case ($-2 < z/L < 0$)

$$- \frac{f C_{iw}(f)}{u_*^2} = \frac{12 n}{(1 + 9.6 n)^{7/3}}, \quad (2.126)$$

$$-\frac{f C_{wT}(f)}{u_* T_*} = \left\{ \begin{array}{ll} \frac{11n}{(1+13.3n)^{7/4}} & \text{for } n \leq 1.0 \\ \frac{4n}{(1+3.8n)^{7/3}} & \text{for } n > 1.0 \end{array} \right\}, \quad (2.127)$$

and for the stable case ($0 < z/L < 2$):

$$-\frac{f C_{uw}(f)}{u_*^2} = 0.05 n^{-4/3} \left(1 + 7.9 \frac{z}{L}\right) \quad (2.128)$$

$$-\frac{f C_{wT}(f)}{u_* T_*} = 0.14 n^{-4/3} \left(1 + 6.4 \frac{z}{L}\right) \quad (2.129)$$

A log–log plot of $f S_X(f)$ versus f (see e.g. Figure 2.12) can be used to illustrate the power law relationships in the form $f S_X(f) \approx f^{-2/3}$ and $S_X(f) \approx f^{-5/3}$ (X is an arbitrary parameter). In a linear-linear plot of $S_X(f)$ versus f , the area below the graph in the range Δf is equal to the standard deviation $\sigma_A(\Delta f)$. The resolution at low frequencies is often bad. In a log-linear plot the area below the graph of $f \cdot S_X(f)$ versus f , is equal to the energy density. The multiplication of the values of the ordinate by f and logarithmic abscissa, gives a better representation of the low frequencies.

Figure 2.12 illustrates that the frequency of the energy maximum of the spectra is one order larger for the vertical than for the horizontal wind velocity. Accordingly, vertically moving turbulence elements are smaller and have a higher frequency than horizontally moving turbulence elements.

An alternative statistical parameter to the autocorrelation function, Eq. (2.112), is the structure function. It is a relation between the value of a variable at time t , $X(t)$, and its value at a later time, $X(t+L)$, note L is not the Obukhov length. If the time between the measurements is ΔT , then $L = j \Delta T$ and

$$D_{XX}(L) = \frac{1}{N} \sum_{k=0}^{N-j} (X_k - X_{k+j})^2. \quad (2.130)$$

If simultaneous measurements are made at several locations, the structure function can be computed using $L = j \Delta r$ where Δr is the spatial separation between measurement sites.

The energy density in the inertial sub-range according to Eq. (2.112) can also be determined using the structure function (Tatarski 1961), which is with the spatial distance r

$$D_u(r) = c_u \varepsilon^{2/3} r^{2/3}, \quad (2.131)$$

with the structure constant $c_u \sim 4.02 \beta_u$, $\beta_u \sim 0.5$ (Sreenivasan 1995), and the structure function parameter

$$C_u^2 = c_u \varepsilon^{2/3}. \quad (2.132)$$

The structure function for the temperature is given by

$$D_T(r) = c_T N_T \varepsilon^{-1/3} r^{2/3}, \quad (2.133)$$

with the structure constant $c_T \sim 4.02 \beta_T$, with β_T Obukhov-Corrsin constant (Obukhov 1949; Corrsin 1951), and the structure function parameter

$$C_T^2 = c_T N_T \varepsilon^{-1/3}. \quad (2.134)$$

The Obukhov-Corrsin constant is about 0.4 (Sreenivasan 1996). The ratio β_T/β_u is equal to the turbulent Prandtl number.

The structure function for moisture is given by

$$D_q(r) = c_q N_q \varepsilon^{-1/3} r^{2/3}, \quad (2.135)$$

with the structure constant $c_q \sim 4.02 \beta_q$ and the structure function parameter

$$C_q^2 = c_q N_q \varepsilon^{-1/3}. \quad (2.136)$$

The structure function parameters are very relevant for meteorological measuring techniques (Kohsiek 1982; Beyrich et al. 2005), because they are directly connected to the refraction structure function parameter C_n^2 (Hill et al. 1980),

$$C_n^2 = \left(79.2 \cdot 10^{-6} \frac{p}{T^2}\right)^2 C_T^2 \quad (2.137)$$

which is proportional to the backscatter echo of ground-based remote sensing techniques:

$$C_n^2 = A^2 C_T^2 + 2ABC_{Tq} + B^2 C_q^2 \quad (2.138)$$

The coefficients A and B are dependent on temperature, humidity, pressure and the electromagnetic wave length (Hill et al. 1980; Andreas 1989; Beyrich et al. 2005). While a dependence on temperature and humidity exists for microwaves, the humidity dependence on visible and near infrared light is negligible.

The stability dependence of the structure function parameter is given by a dimensionless function of the energy dissipation, which has the character of a universal function (Wyngaard et al. 1971b). For the surface layer, they are given in the form (Kaimal and Finnigan 1994):

$$\frac{C_u^2 z^{2/3}}{u_*^2} = \begin{cases} 4\left(1 + 0.5 \frac{z}{L}\right)^{2/3} & \text{for } z/L \leq 0 \\ 4\left(1 + 5 \frac{z}{L}\right)^{2/3} & \text{for } z/L > 0 \end{cases} \quad (2.139)$$

$$\frac{C_T^2 z^{2/3}}{T_*^2} = \begin{cases} 5\left(1 + 6.4 \frac{z}{L}\right)^{-2/3} & \text{for } z/L \leq 0 \\ 5\left(1 + 3 \frac{z}{L}\right) & \text{for } z/L > 0 \end{cases} \quad (2.140)$$

Other universal functions are listed in Appendix A.4. These will be used later for the determination of the sensible heat flux with scintillometers (see Sect. 6.2.5). Within the range of uncertainties of the measurements, all functions for C_T^2 can be applied.

The temperature structure function parameter C_T^2 can be determined according to Wyngaard et al. (1971b) by the vertical temperature profile

$$C_T^2 = z^{-4/3} (\partial\theta/\partial z)^2 f_T(Ri) \quad (2.141)$$

with the empirical stability function $f_T(Ri)$.

2.6 Atmospheric Boundary Layer

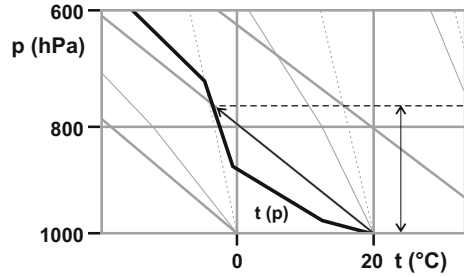
Even though micrometeorological measurements and modelling primarily focus on the surface layer it could be shown that the characteristics of the atmospheric boundary layer are important for many processes. As an example, the mixed-layer depth limits the vertical mixing of emissions. Therefore, in the following a short overview of the determination of the mixed layer height and of boundary-layer profile relationships is presented. More in-depth descriptions are given in the literature (Stull 1988; Garratt 1992; Jacobson 2005; Kraus 2008).

2.6.1 Mixed Layer Height

For practical issues the boundary-layer height, which includes the capping inversion and entrainment layer, is less important than the mixed-layer height. In the mixed layer (see Sect. 1.3), emissions from the surface and any material passing through the entrainment layer are mixed by convection and mechanical turbulence at time scales of about 1 h (Seibert et al. 2000). However, there is no standard method available to determine the mixed-layer height. Several observational methods and modelling approaches have been adopted.

Traditional methods use data from radiosondes, but can also be applied to observations from tethered balloons and aircrafts. For convective conditions, the

Fig. 2.13 Determination of the mixed layer height with the parcel method using the thermodynamic diagram



simplest method is the parcel method (Holzworth 1964, 1967). It is assumed that an air parcel lifts up adiabatically in the unstable boundary layer up to a level, where the surrounding potential temperature is warmer than those of the parcel (Fig. 2.13). One shortcoming of this method is finding the right surface temperature due to strong vertical temperature gradients near the surface. For instance, Troen and Mahrt (1986) proposed to apply an additional correction term to the surface temperature. According to Seibert et al. (2000) the same effect is achieved by using the virtual potential temperature of the surface level. A method proposed by Busch et al. (1976) and applied by Troen and Mahrt (1986) was operationally implemented by Beyrich and Leps (2012). It based on the calculation of the bulk-Richardson number

$$Ri_B(z) = -z \frac{g}{\theta_0} \cdot \frac{(\theta(z) - \theta_0)}{u(z)^2 + v(z)^2}. \quad (2.142)$$

The mixed-layer height is the level where Ri_B reaches a critical value of about 0.2.

Sounding techniques like sodars and lidars, which can detect temperature inhomogeneities, or strong gradients of moisture or aerosol concentrations, are also suitable to determine the mixed-layer height. However, due to measurement-range limitations, sodars can typically only detect the mixed layer evolution in the morning (Beyrich 1997). Lidars, on the other hand, cannot be applied in the case of low clouds because the backscatter from the cloud base is very strong and areas above the clouds cannot be seen. Recently, it was shown that mixed-layer height can also be reliably estimated with ceilometers, which are widespread to detect cloud base height, if the general shortcomings of lidar techniques are accepted (Münkel et al. 2007). Finally, mixed layer heights determined with remote techniques are in a good agreement with numerical simulations (Helmis et al. 2012).

2.6.2 Resistance Law

Analogue to the surface layer, similarity laws can also be derived for the boundary layer if the geostrophic wind speed u_g is factored in. Besides the roughness length, the Obukhov length and the Coriolis parameter the geostrophic drag coefficient u_*/u_g and the Rossby number,

$$Ro = \frac{u_g}{fz_0}, \quad (2.143)$$

are the scaling parameters (here and in Eq. 2.146 u_g is the mean geostrophic wind velocity and not the component of the geostrophic wind in x -direction like in Eq. 2.11 and the following text). Thus type of scaling is called Rossby number similarity (Garratt 1992; Kraus 2008; Salby 2012; Hantel 2013). On this basis, Kazanski und Monin (1960, 1961) developed a stability parameter for the whole boundary layer

$$\mu = \frac{z_i}{L}, \quad (2.144)$$

with the boundary layer height determined by

$$z_i = \frac{\kappa u_*}{f} \quad (2.145)$$

Furthermore, Kazanski und Monin (1960, 1961) formulated the so-called resistance law, which can be applied for the calculation of wind profiles:

$$\ln Ro = A - \ln \frac{u_*}{u_g} + \left[\frac{\kappa^2}{(u_*/u_g)^2} - B^2 \right] \quad (2.146)$$

For both horizontal wind components u_g and v_g (perpendicular to u_g) of the geostrophic wind follows:

$$\frac{u_g}{u_*} = \frac{1}{\kappa} \left(\ln \frac{u_*}{fz_0} - A \right) \quad (2.147)$$

$$\frac{v_g}{u_*} = \frac{B}{\kappa} \quad (2.148)$$

The coefficients A and B are functions of the stability parameter μ .

The resistance law was subject of intensive theoretical and experimental investigations in the 1960s and 1970s (Csanady 1967; Blackadar and Tennekes 1968; Clarke 1970; Wippermann and Yordanov 1972; Clarke and Hess 1974; Zilitinkevich 1970, 1975). Due to high uncertainties in the determination of A and

B and progress in numerical modeling techniques the resistance law is nowadays rarely discussed in textbooks (Blackadar 1997; Kraus 2008). More recently it has however again received attention in wind energy studies that require relatively simple methods to determine the wind profile and wind resource in the whole boundary layer (Gryning et al. 2007; Peña et al. 2010).

2.6.3 Integral Turbulence Characteristics

Integral turbulence characteristics can also be applied above the surface layer. For free convection ($z/L < -1$), scaling with the Deardorff velocity Eq. (2.42) and the mixed layer height, z_i , is necessary (Garratt 1992). Such parameterizations must show the decrease of the integral characteristics with increasing height as well as the increase in the entrainment layer. The following parameterizations were given by Sorbjan (1989, 2008):

$$\sigma_w/w_* = 1.08(z/z_i)^{1/3} (1 - z/z_i)^{1/3} \quad (2.149)$$

$$\sigma_\theta/T_* = 2(z/z_i)^{-2/3} (1 - z/z_i)^{4/3} + 0.94(z/z_i)^{4/3} (1 - z/z_i)^{-2/3} \quad (2.150)$$

References

- Amiro BD (1990) Comparison of turbulence statistics within three boreal forest canopies. *Boundary-Layer Meteorol.* 51:99–121.
- Andreas EL (1989) Two-wavelength method of measuring path-averaged turbulent surface heat fluxes. *J Atm Oceanic Techn.* 6:280–292.
- Andreas EL (2002) Parametrizing scalar transfer over snow and ice: A review. *J Hydrometeorol.* 3:417–432.
- Andreas EL, Claffey KJ, Fairall CW, Grachev AA, Guest PS, Jordan RE and Persson POG (2004) Measurements of the von Kármán constant in the atmospheric surface layer - further discussions. 16th Conference on Boundary Layers and Turbulence, Portland ME2004. *Am. Meteorol. Soc.*, pp. 1–7, paper 7.2.
- Arya SP (1999) *Air Pollution Meteorology and Dispersion*. Oxford University Press, New York, Oxford, 310 pp.
- Arya SP (2001) *Introduction to Micrometeorology*. Academic Press, San Diego, 415 pp.
- Beljaars ACM (1995) The parametrization of surface fluxes in large scale models under free convection. *Quart J Roy Meteorol Soc.* 121:255–270.
- Berkowicz R and Prahm LP (1984) Spectral representation of the vertical structure of turbulence in the convective boundary layer. *Quart J Roy Meteorol Soc.* 110:35–52.
- Bernhardt K-H (1995) Zur Interpretation der Monin-Obuchovschen Länge. *Meteorol Z.* 4:81–82.
- Bernhardt K (1970) Der ageostrophische Massenfluß in der Bodenreibungsschicht bei beschleunigungsfreier Strömung. *Z Meteorol.* 21:259–279.
- Bernhardt K (1972) Vorlesung ‘Dynamik der Atmosphäre’. Humboldt-Universität zu Berlin
- Bernhardt K (1975) Some characteristics of the dynamic air-surface interaction in Central Europe. *Z Meteorol.* 25:63–68.

- Bernhardt K (1980) Zur Frage der Gültigkeit der Reynoldsschen Postulate. *Z Meteorol.* 30:361–368.
- Beyrich F (1997) Mixing height estimation from sodar data — A critical discussion. *Atmos Environm.* 31:3941–3953.
- Beyrich F, Kouznetsov RD, Leps J-P, Lüdi A, Meijninger WML and Weisensee U (2005) Structure parameters for temperature and humidity from simultaneous eddy-covariance and scintillometer measurements. *Meteorol Z.* 14:641–649.
- Beyrich F and Leps J-P (2012) An operational mixing height data set from routine radiosoundings at Lindenberg: Methodology. *Meteorol Z.* 21:337–348.
- Blackadar AK and Tennekes H (1968) Asymptotic similarity in neutral barotropic planetary boundary layers. *J Atmos Sci.* 25:1015–1020.
- Blackadar AK (1997) *Turbulence and Diffusion in the Atmosphere.* Springer, Berlin, Heidelberg, 185 pp.
- Boussinesq J (1877) *Essai sur la théorie des eaux courantes.* Mem Savants Etrange. 23:46 pp.
- Bowen IS (1926) The ratio of heat losses by conduction and by evaporation from any water surface. *Phys Rev.* 27:779–787.
- Brocks K and Krügermeyer L (1970) Die hydrodynamische Rauigkeit der Meeresoberfläche. *Ber Inst Radiometeorol Marit Meteorol.* 14:55 pp.
- Buckingham E (1914) On physically similar systems; illustrations of the use of dimensional equations. *Phys Rev.* 4:345–376.
- Busch NE, Chang SW and Anthes RA (1976) A Multi-Level Model of the Planetary Boundary Layer Suitable for Use with Mesoscale Dynamic Models. *J Appl Meteorol.* 15:909–919.
- Businger JA and Yaglom AM (1971) Introduction to Obukhov's paper "Turbulence in an atmosphere with a non-uniform temperature". *Boundary-Layer Meteorol.* 2:3–6.
- Businger JA, Wyngaard JC, Izumi Y and Bradley EF (1971) Flux-profile relationships in the atmospheric surface layer. *J Atmos Sci.* 28:181–189.
- Businger JA (1982) Equations and concepts. In: Nieuwstadt FTM and Van Dop H (eds.), *Atmospheric turbulence and air pollution modelling: A course held in The Hague, 21–25 September 1981.* D. Reidel Publ. Co., Dordrecht, 1–36.
- Businger JA (1986) Evaluation of the accuracy with which dry deposition can be measured with current micrometeorological techniques. *J Appl Meteorol.* 25:1100–1124.
- Businger JA (1988) A note on the Businger-Dyer profiles. *Boundary-Layer Meteorol.* 42:145–151.
- Charnock H (1955) Wind stress on water surface. *Quart J Roy Meteorol Soc.* 81:639–642.
- Cheng Y and Bruntseart W (2005) Flux-profile relationships for wind speed and temperature in the stable atmospheric boundary layer. *Boundary-Layer Meteorol.* 114:519–538.
- Clarke RH (1970) Observational studies in the atmospheric boundary layer. *Quart J Roy Meteorol Soc.* 96:91–114.
- Clarke RH and Hess GD (1974) Geostrophic departure and the functions A and B of Rossby-number similarity theory. *Boundary-Layer Meteorol.* 7:267–287.
- Corsin S (1951) On the spectrum of isotropic temperature fluctuations in an isotropic turbulence. *J Appl Phys.* 22:469–473.
- Csanady GT (1967) On the "resistance law" of a turbulent Ekman-Layer. *J Atmos Sci.* 24:467–471.
- Davenport AG, Grimmond CSB, Oke TR and Wieringa J (2000) Estimating the roughness of cities and sheltered country. 12th Conference on Applied Climatology, Asheville, NC2000. American Meteorological Society, pp. 96–99.
- Deardorff JW (1966) The counter-gradient heat flux in the lower atmosphere and in the laboratory. *J Atmos Sci.* 23:503–506.
- Deardorff JW (1970) Convective Velocity and Temperature Scales for the Unstable Planetary Boundary Layer and for Rayleigh Convection. *J Atmos Sci.* 27:1211–1213.
- Dyer AJ (1974) A review of flux-profile-relationships. *Boundary-Layer Meteorol.* 7:363–372.
- ESDU (1972) Characteristics of wind speed in the lowest layers of the atmosphere near the ground: strong winds. *Engl. Sci. Data Unit Ltd. Regent St., London*, 35 pp.
- Etling D (2008) *Theoretische Meteorologie.* Springer, Berlin, Heidelberg, 376 pp.

- Foken T (1990) Turbulenter Energieaustausch zwischen Atmosphäre und Unterlage - Methoden, meßtechnische Realisierung sowie ihre Grenzen und Anwendungsmöglichkeiten. Ber Dt Wetterdienstes. 180:287 pp.
- Foken T, Skeib G and Richter SH (1991) Dependence of the integral turbulence characteristics on the stability of stratification and their use for Doppler-Sodar measurements. *Z Meteorol.* 41:311–315.
- Foken T, Jegede OO, Weisensee U, Richter SH, Handorf D, Görsdorf U, Vogel G, Schubert U, Kirzel H-J and Thiermann V (1997) Results of the LINEX-96/2 Experiment. Dt Wetterdienst, Forsch. Entwicklung, Arbeitsergebnisse. 48:75 pp.
- Foken T (2006) 50 years of the Monin-Obukhov similarity theory. *Boundary-Layer Meteorol.* 119:431–447.
- Garratt JR (1992) *The Atmospheric Boundary Layer*. Cambridge University Press, Cambridge, 316 pp.
- Gryning S-E, Batchvarova E, Brümmner B, Jørgensen H and Larsen S (2007) On the extension of the wind profile over homogeneous terrain beyond the surface boundary layer. *Boundary-Layer Meteorol.* 124:251–268.
- Handorf D, Foken T and Kottmeier C (1999) The stable atmospheric boundary layer over an Antarctic ice sheet. *Boundary-Layer Meteorol.* 91:165–186.
- Hantel M (2013) *Einführung Theoretische Meteorologie*. Springer Spektrum, Berlin, Heidelberg, 430 pp.
- Hasager CB and Jensen NO (1999) Surface-flux aggregation in heterogeneous terrain. *Quart J Roy Meteorol Soc.* 125:2075–2102.
- Helmis CG, Sgouros G, Tombrou M, Schäfer K, Münkel C, Bossioli E and Dandou A (2012) A comparative study and evaluation of mixing-height estimation based on sodar-RASS, ceilometer data and numerical model simulations. *Boundary-Layer Meteorol.* 145:507–526.
- Hill RJ, Clifford SF and Lawrence RS (1980) Refractive index and absorption fluctuations in the infrared caused by temperature, humidity and pressure fluctuations. *J Opt Soc Am.* 70:1192–1205.
- Högström U (1974) A field study of the turbulent fluxes of heat water vapour and momentum at a 'typical' agricultural site. *Quart J Roy Meteorol Soc.* 100:624–639.
- Högström U (1985) Von Kármán constant in atmospheric boundary flow: Reevaluated. *J Atmos Sci.* 42:263–270.
- Högström U (1988) Non-dimensional wind and temperature profiles in the atmospheric surface layer: A re-evaluation. *Boundary-Layer Meteorol.* 42:55–78.
- Högström U (1990) Analysis of turbulence structure in the surface layer with a modified similarity formulation for near neutral conditions. *J Atmos Sci.* 47:1949–1972.
- Högström U (1996) Review of some basic characteristics of the atmospheric surface layer. *Boundary-Layer Meteorol.* 78:215–246.
- Högström U, Hunt JCR and Smedman A-S (2002) Theory and measurements for turbulence spectra and variances in the atmospheric neutral surface layer. *Boundary-Layer Meteorol.* 103:101–124.
- Højstrup J (1981) A simple model for the adjustment of velocity spectra in unstable conditions downstream of an abrupt change in roughness and heat flux. *Boundary-Layer Meteorol.* 21:341–356.
- Holzworth GC (1964) Estimates of mean maximum mixing depth in the contiguous United States. *Monthly Weather Review.* 92:235–242.
- Holzworth GC (1967) Mixing depths, wind speeds and air pollution potential for selected locations in the United States. *J Appl Meteorol.* 6:1039–1044.
- Jacobson MZ (2005) *Fundamentals of Atmospheric Modelling*. Cambridge University Press, Cambridge, 813 pp.
- Johansson C, Smedman A, Högström U, Brasseur JG and Khanna S (2001) Critical test of Monin-Obukhov similarity during convective conditions. *J Atmos Sci.* 58:1549–1566.
- Kader BA and Yaglom AM (1972) Heat and mass transfer laws for fully turbulent wall flows. *Int J Heat Mass Transfer.* 15:2329–2350.

- Kaimal JC, Wyngaard JC, Izumi Y and Coté OR (1972) Spectral characteristics of surface layer turbulence. *Quart J Roy Meteorol Soc.* 98:563–589.
- Kaimal JC and Finnigan JJ (1994) *Atmospheric Boundary Layer Flows: Their Structure and Measurement.* Oxford University Press, New York, NY, 289 pp.
- Kantha LH and Clayson CA (2000) *Small scale processes in geophysical fluid flows.* Academic Press, San Diego, 883 pp.
- Kazanski AB and Monin AS (1960) A turbulent regime above the surface atmospheric layer (in Russian). *Izv AN SSSR, ser Geofiz.* 1:165–168.
- Kazanski AB and Monin AS (1961) On the dynamical interaction between the atmosphere and the Earth's surface (in Russian). *Izv AN SSSR, ser Geofiz.* 5:786–788.
- Kitajgorodskij SA and Volkov JA (1965) O rascete turbulentnych potokov tepla i vlagi v privodnom sloe atmosfery (The calculation of the turbulent fluxes of temperature and humidity in the atmosphere near the water surface) *Izv AN SSSR, Fiz Atm Okeana.* 1:1317–1336.
- Kitajgorodskij SA (1976) Die Anwendung der Ähnlichkeitstheorie für die Bearbeitung der Turbulenz in der bodennahen Schicht der Atmosphäre. *Z Meteorol.* 26:185–204.
- Kohsiek W (1982) Measuring C_T^2 , C_Q^2 , and C_{TQ} in the unstable surface layer, and relations to the vertical fluxes of heat and moisture. *Boundary-Layer Meteorol.* 24:89–107.
- Kolmogorov AN (1941a) Rassejanie energii pri lokalno-isotropoi turbulentnosti (Dissipation of energy in locally isotropic turbulence). *Dokl AN SSSR.* 32:22–24.
- Kolmogorov AN (1941b) Lokalnaja struktura turbulentnosti v neschtschimaemoi schidkosti pri otschen bolschich tshislach Reynoldsa (The local structure of turbulence in incompressible viscous fluid for very large Reynolds numbers). *Dokl AN SSSR.* 30:299–303.
- Kondo J and Sato T (1982) The determination of the von Kármán constant. *J Meteor Soc Japan.* 60:461–471.
- Kramm G and Herbert F (2009) Similarity hypotheses for the atmospheric surface layer expressed by non-dimensional characteristic invariants – A review *Open Atmos Sci J.* 3:48–79.
- Kraus H (2004) *Die Atmosphäre der Erde.* Springer, Berlin, Heidelberg, 422 pp.
- Kraus H (2008) *Grundlagen der Grenzschichtmeteorologie.* Springer, Berlin, Heidelberg, 211 pp.
- Lettau HH (1957) Windprofil, innere Reibung und Energieumsatz in den untersten 500 m über dem Meer. *Beitr Phys Atm.* 30:78–96.
- Lumley JL and Panofsky HA (1964) *The structure of atmospheric turbulence.* Interscience Publishers, New York, 239 pp.
- Monin AS and Obukhov AM (1954) Osnovnye zakonomernosti turbulentnogo peremesivaniya v prizemnom sloe atmosfery (Basic laws of turbulent mixing in the atmosphere near the ground). *Trudy Geofiz inst AN SSSR.* 24 (151):163–187.
- Monin AS and Yaglom AM (1973) *Statistical Fluid Mechanics: Mechanics of Turbulence, Volume 1.* MIT Press, Cambridge, London, 769 pp.
- Monin AS and Yaglom AM (1975) *Statistical Fluid Mechanics: Mechanics of Turbulence, Volume 2.* MIT Press, Cambridge, London, 874 pp.
- Münkel C, Eresmaa N, Räsänen J and Karppinen A (2007) Retrieval of mixing height and dust concentration with lidar ceilometer. *Boundary-Layer Meteorol.* 124:117–128.
- Obukhov AM (1946) Turbulentnost' v temperaturnoj - neodnorodnoj atmosfere (Turbulence in an atmosphere with a non-uniform temperature). *Trudy Inst Theor Geofiz AN SSSR* 1:95–115.
- Obukhov AM (1949) Struktura temperaturnogo polja v turbulentnom potoke (Structure of the temperature field in the turbulent stream). *Izv AN SSSR, ser geogr geofiz.* 13:58–69.
- Oncley SP, Friehe CA, Larue JC, Businger JA, Itsweire EC and Chang SS (1996) Surface-layer fluxes, profiles, and turbulence measurements over uniform terrain under near-neutral conditions. *J Atmos Sci.* 53:1029–1054.
- Paeschke W (1937) Experimentelle Untersuchungen zum Rauigkeitsproblem in der bodennahen Luftschicht. *Z Geophys.* 13:14–21.
- Pandolfo JP (1966) Wind and temperature profiles for constant-flux boundary layers in lapse conditions with a variable eddy conductivity to eddy viscosity ratio. *J Atmos Sci.* 23:495–502.
- Panofsky HA (1963) Determination of stress from wind and temperature measurements. *Quart J Roy Meteorol Soc.* 89:85–94.

- Panofsky HA, Tennekes H, Lenschow DH and Wyngaard JC (1977) The characteristics of turbulent velocity components in the surface layer under convective conditions. *Boundary-Layer Meteorol.* 11:355–361.
- Panofsky HA and Dutton JA (1984) *Atmospheric Turbulence - Models and Methods for Engineering Applications*. John Wiley and Sons, New York, 397 pp.
- Paulson CA (1970) The mathematical representation of wind speed and temperature profiles in the unstable atmospheric surface layer. *J Climate Appl Meteorol.* 9:857–861.
- Peltier LJ, Wyngaard JC, Khanna S and Brasseur JG (1996) Spectra in the unstable surface layer. *J Atmos Sci.* 53:49–61.
- Peña A, Gryning S-E and Hasager C (2010) Comparing mixing-length models of the diabatic wind profile over homogeneous terrain. *Theor Appl Climat.* 100:325–335.
- Prandtl L (1925) Bericht über Untersuchungen zur ausgebildeten Turbulenz. *Z Angew Math Mech.* 5:136–139.
- Pruitt WO, Morgan DL and Lourence FJ (1973) Momentum and mass transfer in the surface boundary layer. *Quart J Roy Meteorol Soc.* 99:370–386.
- Reithmaier LM, Göckede M, Markkanen T, Knohl A, Churkina G, Rebmann C, Buchmann N and Foken T (2006) Use of remotely sensed land use classification for a better evaluation of micrometeorological flux measurement sites. *Theor Appl Climat.* 84:219–233.
- Roll HU (1948) Wassernahes Windprofil und Wellen auf dem Wattenmeer. *Ann Meteorol.* 1:139–151.
- Salby ML (2012) *Physics of the Atmosphere and Climate*. Cambridge University Press, Cambridge, 666 pp.
- Schlichting H and Gersten K (2003) *Boundary-Layer Theory*. McGraw Hill, New York, XXIII, 799 pp.
- Schmitz-Peiffer A, Heinemann D and Hasse L (1987) The ageostrophic methode - an update. *Boundary-Layer Meteorol.* 39:269–281.
- Seibert P, Beyrich F, Gryning S-E, Joffre S, Rasmussen A and Tercier P (2000) Review and intercomparison of operational methods for the determination of the mixing height. *Atmos Environm.* 34:1001–1027.
- Skeib G (1980) Zur Definition universeller Funktionen für die Gradienten von Windgeschwindigkeit und Temperatur in der bodennahen Luftschicht. *Z Meteorol.* 30:23–32.
- Smedman A-S (1991) Some turbulence characteristics in stable atmospheric boundary layer flow. *J Atmos Sci.* 48:856–868.
- Sonntag D (1990) Important new values of the physical constants of 1986, vapour pressure formulations based on the ITC-90, and psychrometer formulae. *Z Meteorol.* 40:340–344.
- Sorbjan Z (1989) *Structure of the Atmospheric Boundary Layer*. Prentice Hall, New York, 317 pp.
- Sorbjan Z (2008) Gradient-based similarity in the atmospheric boundary layer. *Acta Geophys.* 56:220–233.
- Sreenivasan KR (1995) On the universality of the Kolmogorov constant. *Phys Fluids.* 7:2778–2784.
- Sreenivasan KR (1996) The passive scalar spectrum and the Obukhov–Corrsin constant. *Phys Fluids.* 8:189–196.
- Stull RB (1984) Transilient turbulence theorie, Part I: The concept of eddy mixing across finite distances. *J Atmos Sci.* 41:3351–3367.
- Stull RB (1988) *An Introduction to Boundary Layer Meteorology*. Kluwer Acad. Publ., Dordrecht, Boston, London, 666 pp.
- Stull RB (2000) *Meteorology for Scientists and Engineers*. Brooks/Cole, Pacific Grove, 502 pp.
- Tatarski VI (1961) *Wave Propagation in a Turbulent Medium*. McGraw-Hill, New York, 285 pp.
- Taylor GI (1938) The spectrum of turbulence. *Proceedings Royal Society London.* A 164:476–490.
- Tennekes H (1982) Similarity relations, scaling laws and spectral dynamics. In: Nieuwstadt FTM and Van Dop H (eds.), *Atmospheric turbulence and air pollution modelling*. D. Reidel Publ. Comp., Dordrecht, Boston, London, 37–68.

- Thomas C and Foken T (2002) Re-evaluation of integral turbulence characteristics and their parameterisations. 15th Conference on Turbulence and Boundary Layers, Wageningen, NL, 15–19 July 2002. *Am. Meteorol. Soc.*, pp. 129–132.
- Tillman JE (1972) The indirect determination of stability, heat and momentum fluxes in the atmospheric boundary layer from simple scalar variables during dry unstable conditions. *J Climate Appl Meteorol.* 11:783–792.
- Troen I and Lundtang Peterson E (1989) *European Wind Atlas*. Risø National Laboratory, Roskilde, 656 pp.
- Troen IB and Mahrt L (1986) A simple model of the atmospheric boundary layer; sensitivity to surface evaporation. *Boundary-Layer Meteorol.* 37:129–148.
- Wieringa J (1980) A reevaluation of the Kansas mast influence on measurements of stress and cup anemometer over speeding. *Boundary-Layer Meteorol.* 18:411–430.
- Wieringa J (1992) Updating the Davenport roughness classification. *J Wind Eng Industry Aerodyn.* 41:357–368.
- Wippermann F and Yordanov D (1972) A note on the Rossby similarity for flows of barotropic planetary boundary layers. *Beitr Phys Atm.* 45:66–71.
- Wyngaard JC, Coté OR and Izumi Y (1971a) Local free convection, similarity and the budgets of shear stress and heat flux. *J Atmos Sci.* 28:1171–1182.
- Wyngaard JC and Coté OR (1971) The budgets of turbulent kinetic energy and temperature variance in the atmospheric surface layer. *J Atmos Sci.* 28:190–201.
- Wyngaard JC, Izumi Y and Collins SA (1971b) Behavior of the refractive-index-structure parameter near the ground. *J Opt Soc Am.* 61:1646–1650.
- Wyngaard JC (1973) On surface layer turbulence. In: Haugen DH (ed.), *Workshop on Micrometeorology*. *Am. Meteorol. Soc.*, Boston, 101–149.
- Wyngaard JC (2010) *Turbulence in the Atmosphere*. Cambridge University Press, Cambridge, 393 pp.
- Yaglom AM (1977) Comments on wind and temperature flux-profile relationships. *Boundary-Layer Meteorol.* 11:89–102.
- Yaglom AM (1979) Similarity laws for constant-pressure and pressure-gradient turbulent wall flow. *Ann Rev Fluid Mech.* 11:505–540.
- Zilitinkevich SS and Tschalikov DV (1968) Opređenje universalnych profilej skorosti vetra i temperatury v prizemnom sloe atmosfery (Determination of universal profiles of wind velocity and temperature in the surface layer of the atmosphere). *Izv AN SSSR, Fiz Atm Okeana.* 4:294–302.
- Zilitinkevich SS (1969) On the computation of the basic parameters of the interaction between the atmosphere and the ocean. *Tellus.* 21:17–24.
- Zilitinkevich SS (1970) Dinamika pograničnogo sloia atmosfery (Dynamics of the atmospheric boundary layer). *Gidrometeorologicheskoe Izdatelstvo, Leningrad* pp.
- Zilitinkevich SS (1975) Resistance laws and prediction equations for the depth of the planetary boundary layer. *J Atmos Sci.* 32:741–752.
- Zilitinkevich SS, Perov VL and King JC (2002) Near-surface turbulent fluxes in stable stratification: Calculation techniques for use in general circulation models. *Quart J Roy Meteorol Soc.* 128:1571–1587.